Neurobiology of Disease 96 (2016) 156–170

Contents lists available at ScienceDirect

Neurobiology of Disease

journal homepage: www.elsevier.com/locate/ynbdi

Validation of an improved scale for rating L-DOPA-induced dyskinesia in the mouse and effects of specific dopamine receptor antagonists

Irene Sebastianutto [a,*], Natallia Maslava [a], Corey R. Hopkins [b], M. Angela Cenci [a,*]

[a] Basal Ganglia Pathophysiology Unit, Dept. Exp. Medical Science, Lund University, BMC, 221 84 Lund, Sweden
[b] Department of Pharmaceutical Sciences, College of Pharmacy, University of Nebraska Medical Center, Omaha, NE 68198-6125, USA

ARTICLE INFO

Article history:
Received 19 July 2016
Revised 24 August 2016
Accepted 1 September 2016
Available online 2 September 2016

Keywords:
Parkinson's disease
Movement disorders
Dystonia
Rodent models
Experimental therapeutics

ABSTRACT

Rodent models of L-DOPA-induced dyskinesia (LID) are essential to investigate pathophysiological mechanisms and treatment options. Ratings of abnormal involuntary movements (AIMs) are used to capture both qualitative and quantitative features of dyskinetic behaviors. Thus far, validated rating scales for the mouse have anchored the definition of severity to the time during which AIMs are present. Here we have asked whether the severity of axial, limb, and orolingual AIMs can be objectively assessed with scores based on movement amplitude. Mice sustained 6-OHDA lesions in the medial forebrain bundle and were treated with L-DOPA (3–6 mg/kg/day) until they developed stable AIMs scores. Two independent investigators rated AIM severity using both the validated time-based scale and a novel amplitude scale, evaluating the degree of deviation of dyskinetic body parts relative to their resting position. The amplitude scale yielded a high degree of consistency both within- and between raters. Thus, time-based scores, amplitude scores, and a combination of the two ('global AIM scores') were applied to compare antidyskinetic effects produced by amantadine and by the following subtype-specific DA receptor antagonists: SCH23390 (D1/D5), Raclopride (D2/D3), PG01037 (D3), L-745,870 (D4), and VU6004461 (D4). SCH23390 and Raclopride produced similarly robust reductions in both time-based scores and amplitude scores, while PG01037 and L-745,870 had more partial effects. Interestingly, a novel and highly brain penetrable D4 receptor antagonist (VU6004461) markedly attenuated both time-based and amplitude scores without diminishing the general motor stimulant effect of L-DOPA. In summary, our results show that a dyskinesia scale combining a time dimension with an amplitude dimension ('global AIMs') is more sensitive than unidimensional scales. Moreover, the antidyskinetic effects produced by two chemically distinct D4 antagonists identify the D4 receptor as a potential future target for the treatment of LID.

1. Introduction

The dopamine (DA) precursor 3,4-dihydroxyphenyl-L-alanine (L-DOPA) is the most effective treatment for Parkinson's disease (PD). However, this treatment is prone to induce motor complications (reviewed in Cenci et al., 2011; Salat and Tolosa, 2013). A prominent complication is L-DOPA-induced dyskinesia (LID), abnormal involuntary movements (AIMs) with both choreiform and dystonic components (Manson et al., 2012) that affect the majority of PD patients (Ahlskog and Muenter, 2001; Hauser et al., 2007). LID has a negative impact on quality of life (Hechtner et al., 2014), and represents a serious obstacle to the management of PD as it imposes reductions and fractionations of L-DOPA dosage, limiting the treatment's efficacy. Thus, preventing or reducing LID without compromising the beneficial effects of DA replacement therapy is an important goal for current PD research.

Pathophysiological and therapeutic research on LID is heavily dependent on experimental studies in animal models. These studies have helped reveal pre- and post-synaptic abnormalities in DA transmission at the basis of the movement disorder (Cenci and Lundblad, 2006; Cenci and Konradi, 2010; Cenci, 2014; Fieblinger et al., 2014a; Bastide et al., 2015). In order to identify new potential antidyskinetic drugs, it is advisable to start with a preclinical evaluation in animal models, which not only provide accurate pharmacodynamic information, but can also yield insights into a treatment's mechanisms of action (Bastide et al., 2015). Rodent models are cost-effective, and dyskinesia scales for both rats and mice are now well validated and widely used. In the rat, the most sensitive dyskinesia scale incorporates both a time dimension and a movement amplitude score (Rylander et al., 2010; Breger et al., 2013; Iderberg et al., 2013; Iderberg et al., 2015). Although widely implemented in the rat, a scale based on movement amplitude has not yet been validated in the mouse model of LID. The very rapid movements displayed by dyskinetic mice may pose an obstacle to the

* Corresponding authors.
E-mail addresses: irene.sebastianutto@med.lu.se (I. Sebastianutto), angela.cenci_nilsson@med.lu.se (M.A. Cenci).
Available online on ScienceDirect (www.sciencedirect.com).

http://dx.doi.org/10.1016/j.nbd.2016.09.001
0969-9961/

assessment of movement amplitude during on-line rating sessions (Cenci and Lundblad, 2007). Therefore, both the definition and the assessment of 'dyskinesia amplitude' necessitate careful validation in the mouse.

In this study, we set out to define a new mouse dyskinesia scale based on the degree of deviation of dyskinetic body parts from their resting position ('movement amplitude'). We determined the reliability of this scale by comparing scores given by two independent investigators during on-line rating sessions. Amplitude scores were further validated through off-line analysis of video recordings. We next combined amplitude scores with time-based scores (Lundblad et al., 2004; Lundblad et al., 2005) to generate 'global AIM scores', and examined the sensitivity of this new scale to detect changes in dyskinesia severity produced by several treatments. The latter included a clinically used antidyskinetic medication (amantadine), and experimental treatments targeting specific subtypes of DA receptors (DARs: D1-, D2-, D3- or D4-type DARs). Most of these DAR antagonists had been previously found effective in both non-human primate and rodent models of LID.

2. Materials and methods

2.1. Animals

This study was performed on male C57Bl/6J mice (Charles River/SCANBUR Research A/S; Denmark), approx. 10 weeks old at the beginning of the experiments. Mice were housed under a 12-h light/dark cycle with ad libitum access to water and food. All procedures were approved by the Malmö-Lund Ethical Committee on Animal Research.

2.2. DA-denervating lesion and post-operative care

Unilateral nigrostriatal DA lesions were achieved by injecting 6-hydroxydopamine (6-OHDA) into the medial forebrain bundle (MFB), according to a well-established method (Francardo et al., 2011). Briefly, surgical anesthesia was induced using a mixture of 4% isofluorane in air (Isobavet, Apoteksbolaget) and maintained with 1.2–1.5% isofluorane. Mice were placed in a stereotaxic frame with a mouse adaptor (Kopf Instruments, Tujunga, USA) on a flat skull position. The toxin 6-OHDA-HCl (Sigma Aldrich, Stockholm, Sweden) was dissolved in a 0.02% ascorbic acid-saline solution at a concentration of 3.2 μg/μl (free base concentration). One microliter of this solution was injected at the following coordinates (in mm, relative to bregma and dural surface): AP = −0.7, L = −1.2, DV = −4.7. A glass capillary (outer tip diameter of 50 μm) attached to a 10 μl Hamilton syringe was used for the injections. The injection rate was 0.5 μl/min. The capillary was left in place for 2 min before and 2 min after injection. The analgesic Marcain (bupivacaine, 2.5 mg/ml, AstraZeneca) was injected subcutaneously (10 μl/10 g, body weight) before first skin incision. Postoperative care of the mice was performed as in (Francardo et al., 2011) with some modifications. Briefly, in the first week post-surgery, loss of body temperature was prevented by placing mice overnight in a warm ventilated cabinet (30 °C internal temperature; IVC Recovery Unit; Tecniplast S.P.A., Italy). During the first 2–3 weeks post-surgery mice were rehydrated, as necessary, using sterile glucose/Ringer acetate solution (50 mg/ml, Baxter Medical AB, Sweden; 0.1–0.4 ml/10 g body weight, s.c.) and they received fresh soft dietary gel (DietGel Boost; ClearH_2O, Maine, U.S.A.) in addition to their standard food. The implementation of these procedures afforded a 100% survival rate.

2.3. Cylinder test for drug-free evaluation of 6-OHDA lesion efficacy

Three weeks after 6-OHDA lesion, forelimb use asymmetry was evaluated using the 'cylinder test', which reveals a significant reduction in spontaneous use of the forelimb contralateral to the lesion (Lundblad et al., 2002; Francardo et al., 2011) Briefly, mice were placed individually in a glass cylinder (10 cm diameter and 14 cm height) and were videotaped for 5 min. The total number of supporting wall contacts performed independently with the left and the right forepaw were counted off-line. Wall contacts were defined as events where the animal presses the forepaw with extended digits against the cylinder wall to support its own body weight. Results were expressed as the percentage use of the forelimb contralateral to the lesion (left forepaw contacts over the total number of wall contacts) and 25% contralateral paw usage was used as cut-off value for including mice in the study.

2.4. Experimental design

Fifteen 6-OHDA lesioned mice were treated with L-DOPA for two weeks to induce stable AIM scores. Dyskinesia ratings were performed in parallel, but independently, by two investigators. AIMs were evaluated using both the time-based scale, (originally introduced by Cenci et al., 1998 and herein referred to as 'basic scores') and a new amplitude scale adapted from the rat (Cenci and Lundblad, 2007). Thereafter, the two scores were combined to give a 'global AIM score' (see below). The method was validated by (i) verifying amplitude scores on video recordings; (ii) comparing results from the two raters; (iii) assessing the effects of amantadine, a clinically proven antidyskinetic medication. During the treatment maintenance phase (see below), mice received challenge tests with (i) the D1R antagonist SCH23390; (ii) the D2R antagonist Raclopride; (iii) the D3R antagonist PG01037; (iv) the D4R antagonist L-745,870; (v) the new highly selective D4R antagonist VU6004461. Drug effects on AIMs were evaluated using a randomized cross-over design (Lundblad et al., 2002; Lundblad et al., 2005), allowing wash-out periods of 3 days between drug challenges. Each DAR antagonist was also evaluated using automated tests of horizontal/vertical activity and rotational behavior in an open field. During the drug-testing phase, the stability of AIMs induced by sole L-DOPA treatment (6 mg/kg) was verified by performing 'baseline AIM tests' once a week. Baseline AIMs scores were compared to those recorded upon L-DOPA and vehicle injection ('vehicle + L-DOPA') in each drug challenge test, and no differences were found (data not shown).

2.5. Drug treatments

L-DOPA methyl ester (3 and 6 mg/kg; Sigma Aldrich AB, Sweden) was always coadministered with a fixed dose of Benserazide-HCl (12 mg/kg; Sigma Aldrich AB, Sweden). The drugs were freshly dissolved in physiological saline solution and coadministered s.c. All other drugs used in the study, their doses and administration modalities are reported in Table 1.

During the first two weeks of drug treatment (dyskinesia induction phase), mice received escalating doses of L-DOPA (3 and 6 mg/kg) to induce stable levels of AIMs. At the end of this phase, mice were challenged with amantadine. Throughout the rest of the study, mice were kept on a maintenance regimen of L-DOPA treatment (6 mg/kg, at least twice weekly), and were challenged with DAR antagonists on different weeks.

2.6. Abnormal involuntary movements (AIMs) ratings

Mice were individually placed in transparent plastic cages (18 × 29.5 cm), accommodated on a freestanding metal rack with horizontal shelves. Mice were allowed to habituate to this environment for at least 2 h before the first test, and for 15 min before each subsequent test. During AIMs rating sessions, each mouse was rated online for 1 min every 20 min following L-DOPA injection. On the same monitoring period a GoPro Hero 4 camera was placed in front of the cage for video recording. Dyskinesia was assessed using a well-validated mouse AIMs scale (Lundblad et al., 2002; Lundblad et al., 2005; Francardo et al., 2011), which evaluates AIM severity based on the proportion of observation time during which dyskinetic behaviors are present (Cenci et al.,

Table 1
Drugs, doses and administration procedures used.

Drug	Supplier	Admin. route	Doses (mg/kg)	Vehicle	AIMs test: Adm. Interval to L-DOPA	Main references
Amantadine	Sigma Aldrich	i.p.	40	Saline	100 min	(Lundblad et al., 2002)
SCH23390	Tocris Bioscience	i.p.	0.05 and 0.125	Saline	15 min	(Santini et al., 2009a)
Raclopride	Sigma Aldrich	i.p.	0.05 and 0.250	Saline	15 min	(Santini et al., 2009a)
PG01037	Tocris Bioscience	i.p.	3 and 10	2.5% DMSO + Saline	0 min	(Kumar et al., 2009)
L-745,870	Vanderbilt Center for Neuroscience Drug Discovery	i.p.	1 and 3	Saline	0 min	(Huot et al., 2014)
VU6004461	Vanderbilt Center for Neuroscience Drug Discovery	s.c.	10 and 20	5% Tween80 + Saline	0 min	N.A.

References pertain to studies using the compound together with L-DOPA, and refer to dosage and interval of administration between the two drugs.

1998). The scale considers three topographic subtypes of dyskinetic movements as follows: (i) axial AIMs, i.e. twisting movements of the neck and upper trunk towards the side contralateral to the lesion; (ii) forelimb AIMs, i.e. rapid purposeless movements or dystonic posturing of the contralateral forelimb; (iii) orolingual AIMs, i.e. empty jaw movements, often accompanied by twitching of orofacial muscles and contralateral tongue protrusion. These three AIM subtypes were scored simultaneously on the basic scale according to well-established criteria: 0, no signs of dyskinesia; 1, signs of dyskinesia < 50% of the observation time; 2, dyskinesia during > 50% of the observation time; 3, dyskinesia is continuous, but promptly ceases upon mild visual/auditory stimulation, as produced by opening the cage lid; 4, dyskinesia is continuous and does not cease upon mild visual/auditory stimulation. Half-scores were implemented according to the following definitions: 1.5, dyskinesia is present for 50% of the observation time; 2.5, dyskinesia is virtually continuous, spontaneously ceasing only on one brief occasion, (for very few seconds) during the monitoring period; 3.5, dyskinesia is continuous, and does not promptly cease upon opening the cage lid, but stops for a few seconds when the cage lid closes again. All 15 animals included in the study exhibited basic scores ≥ 2 on at least two AIM subtypes and on at least two monitoring periods per session, and were thus classified as dyskinetic according to previously established definitions (Westin et al., 2006).

The basic scale was combined with a new amplitude scale for mouse AIMs, adapted from an analogous rat scale (Cenci and Lundblad, 2007; Breger et al., 2013). The grading of this scale is summarized in Table 2, and more extensive explanations are given in Results. Briefly, each of the three AIMs subtypes (axial, limb and orolingual; ALO) received an amplitude score from 0 to 4 on each monitoring period. Amplitude was defined both by the degree of deviation of a body part from its natural resting position, and by the number of muscle groups visibly engaged in the dyskinetic movement (Fig. 1). Because hyperkinetic movements can quickly vary during 1-min observation periods, amplitude scores were given so as to represent the most frequent type of movement observed in each animal, allowing also for half-scores to be given (e.g. a score of limb L2.5 was given when mice quickly shifted between L2 and L3). The applicability and reliability of the amplitude AIMs scale was established by two trained investigators, who carried out parallel but independent on-line ratings, obtaining quite similar results. Moreover, amplitude grades were verified by off-line video analysis.

A composite AIM score was then produced by multiplying basic score and amplitude score for each AIM subtype, on each monitoring period. The sum of these scores on one testing session ('global AIMs') could reach a theoretical maximum value of 432.

2.7. Open field

General motor activity (horizontal and vertical activity, and rotational behavior) was evaluated in an open field (50 × 50 cm arena, framed by transparent Plexiglas walls) and recorded using an ANYmaze video tracking system (Stoelting, U.S.A.). Tests were performed during the light phase of the diurnal cycle. Animals were habituated to the open field apparatus for 3 consecutive days before the very first test. Reference values were acquired by treating the mice with (i) vehicle + vehicle (herein referred as 'baseline activity') and (ii) L-DOPA + vehicle. The reference values (for both baseline and L-DOPA-induced activity) were verified before each DAR antagonist challenge. Open field tests were conducted for each DAR antagonist, according to the following procedure. Mice were placed in the center of the box and let habituate for 15 min before injecting either vehicle or one of the DAR antagonists (see Table 1). After an additional 15 min, mice were injected with either vehicle or L-DOPA (6 mg/kg). Following vehicle/L-DOPA injection, mice were recorded for a total of 140 min, and readings were made every 5 min. Parameters measured were the following: (i) distance travelled, (ii) number of rearing events (iii) number of rotations contralateral to the lesion, and (iv) number of ipsilateral rotations.

2.8. Statistical analysis

Statistical analysis was performed using Prism 5 (GraphPad Software). Analysis of variance (ANOVA), factorial or by repeated measures (RM) and post hoc Bonferroni's multiple comparison's test (Bonferroni's test) were used in most cases. Two-group comparisons were made using paired Student's *t*-test (paired *t*-test). The main treatment effects on AIM scores were always verified with non-parametric statistics. Correlations between scores from the two raters were assessed using Pearson's r (presented as r^2 values) and were calculated on the total

Table 2
Definition of amplitude ratings for axial, limb and orolingual AIMs.

AIM subtype	Amplitude score	Description
Axial (A)	A1	Sustained deviation of head/neck by at least 30° (quadrupedal position).
	A2	Sustained deviation of head/neck by at least 60° (quadrupedal position).
	A3	Torsion of neck/upper trunk by at least 90° (bipedal position).
	A4	Torsion of neck/upper trunk by >90° (bipedal position), causing the mouse to lose balance.
Limb (L)	L1	Tiny displacement of the forepaw around a fixed position (e.g. tapping on the floor or small movements about the snout).
	L2	Larger movement causing visible displacement of the whole forelimb, usually to/from snout.
	L3	Large displacement of the whole forelimb with visible engagement of shoulder muscles.
	L4	Vigorous limb displacement, crossing over the midline of the body (animal seems to try and constrain the movement with the non-dyskinetic paw).
Orolingual (O)	O1	Twitching of orofacial muscles and small jaw movements (either lateralized jaw displacements or small jaw openings).
	O2	Visible jaw opening (exposing teeth and tongue), often lateralized.
	O3	Conspicuous jaw opening and occasional tongue protrusion.
	O4	Conspicuous jaw opening, frequent and vigorous tongue protrusion.

Confront descriptions in Table 2 with representations of the axial, limb and orolingual AIM subtypes in Fig. 1.

Fig. 1. Illustration of the AIM amplitude scale developed for the mouse model of LID. A grading scheme from 0 to 4 is applied to each of the main topographic subtypes of dyskinesia (axial AIMs, A0–A4; limb AIMs, L0–L4; and orolingual AIMs, O0–O4). Amplitude grades are here illustrated by means of video photographs, and spelled out using drawings. Please, confront with Table 2.

AIM scores per session (20–180 min) obtained from each individual animal ($n = 15$). Statistical significance was set at $p < 0.05$. F and p values from the ANOVAs are given in figure legends, while post hoc comparisons are reported in both Results and figure legends. Data are presented as group means ± standard errors of the mean (SEM).

3. Results

3.1. Development of a global AIMs scale for the mouse

L-DOPA-induced involuntary movements are phenomenologically similar in mouse and rat (Cenci and Lundblad, 2007). This prompted us to develop a global AIMs scale for the mouse according to the same principles used in the rat (Rylander et al., 2010; Breger et al., 2013; Iderberg et al., 2013; Iderberg et al., 2015). To this end, we first defined a dyskinesia amplitude scale capturing the range of movements seen in this mouse model of LID. The new scale is summarized in Table 2, illustrated in Fig. 1, and explained below.

The amplitude of axial AIMs (grades A1–4) was defined based on the degree of deviation of the neck and upper trunk from their natural resting position (cf. Fig. 1, A0). Axial amplitudes A1 and A2 are usually seen when the animal is in a quadrupedal position and moving on the horizontal plane. Grades A3 and A4 implicate a torsional movement of the upper part of the body, and can only occur when the mouse is in a bipedal position (cf. Fig. 1, panels A3–4). The most severe torsional movements (A4) are usually associated with a loss of balance. In these cases, the mouse abruptly falls down, landing on either the back or the forepaws. Differently from dyskinetic rats (which can sometimes remain lying on their backs for a while), mice tend to recuperate balance immediately after the fall.

The amplitude of limb AIMs (grades L1–4) was defined based on the degree of translocation of the limb contralateral to the lesion from its natural resting position (cf. Fig. 1, panel L0). In the mildest cases (L1), the paw displays hyperkinetic movements of very small amplitude, either tapping on the floor or (most frequently) moving about the snout. Grade L2 refers to sideways limb movements to/from the snout, whereas L3 refers to large forelimb movements with visible engagement of shoulder muscles (in this case too, movements are to/from snout, often alternating with sideways swinging movements). In grade L4, the movement is vigorous and forelimb translocation maximal. As illustrated in Fig. 1, the contralateral limb is displaced across the body's midline. Shoulder extensor muscles are visibly engaged and the non-dyskinetic forelimb frequently moves towards the dyskinetic one (as if attempting to constrain the movement).

The amplitude of orolingual AIMs (O1–4) was defined based on the degree of involvement of facial, masticatory, and lingual muscles relative to a resting state (cf. Fig. 1, O0). The mildest cases (O1–2) manifest as either small jaw openings or brief lateral translocations of the jaw. Grade O2 refers to visible and often lateralized jaw openings, exposing teeth and tongue. Grades O3 and O4 are distinguished by large jaw openings accompanied by a variable degree of tongue protrusion (in O4, tongue protrusion is maximal, see Fig. 1). Among the three subtypes of dyskinesia, orofacial and orolingual AIMs are the most difficult to see and rate (mainly because dyskinetic limb movements often target the snout). In order to provide O1–4 ratings it was fundamental to accommodate the testing cages on racks that allowed for looking at the animal from all angles. We found that the best visualization of orolingual AIMs was often achieved by observing the mouse from below.

Fig. 2 shows results from a representative AIMs test with L-DOPA 6 mg/kg. The scores given by rater #1 and rater #2 were very similar when considering either basic scores (Fig. 2B′, correlation between raters: $r^2 = 0.94$, $p < 0.001$), amplitude scores (Fig. 2C′, correlation between raters: $r^2 = 0.94$, $p < 0.001$) or the combined global scores (Fig. 2A′, correlation between raters: $r^2 = 0.92$, $p < 0.001$). Fig. 2A′, B′ and C′ show the distribution of scores between AIM subtypes, which did not differ between rater #1 and #2 (Fig. 2A′, B′, C′; $p > 0.05$ for each AIM subtype). Next, the suitability of the global AIM scale to detect effects of drugs was verified through challenge tests with amantadine (40 mg/kg), a well-known antidyskinetic medication (Metman et al.,

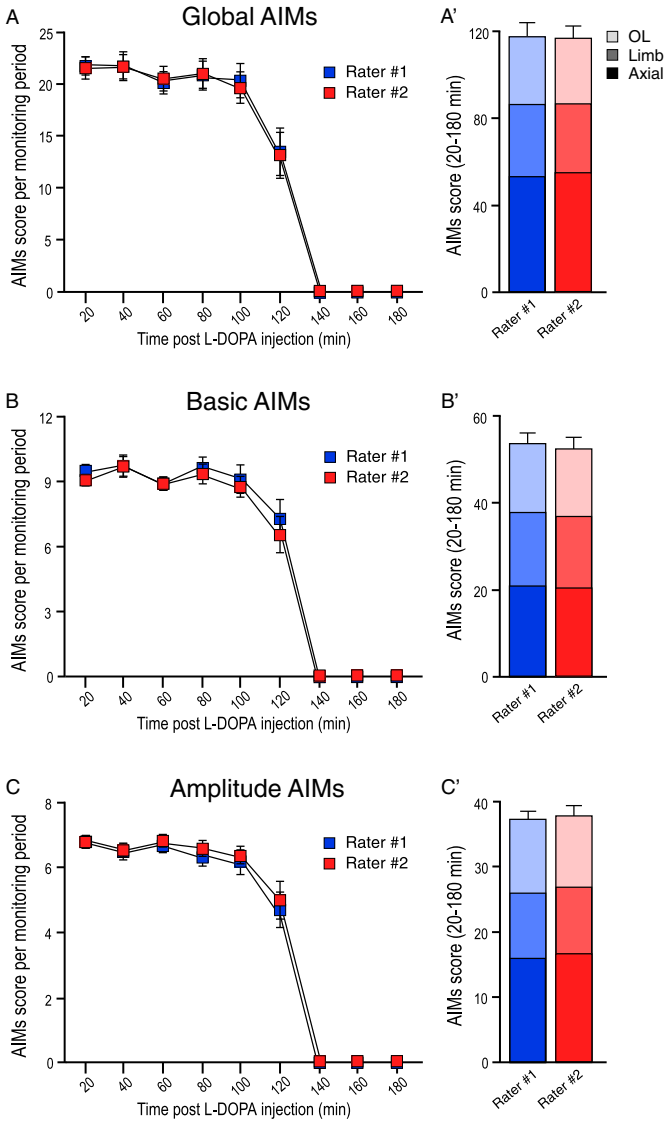

Fig. 2. Validation of the use of global AIMs scale in the mouse model of LID. Involuntary movements were induced in 15 MFB-lesioned mice with 6 mg/kg L-DOPA, and AIMs were rated independently by two investigators. **A**. Time course of global AIM scores within a test session (RM Two-way ANOVA, effect of Rater: $F_{(1,14)} = 0.19$, $p = 0.67$; effect of Time post L-DOPA: $F_{(8,112)} = 123.8$, $p < 0.001$; Interaction: $F_{(8,112)} = 0.32$, $p = 0.95$). **A′**. Sum of global AIMs in one session ($p = 0.67$, $n = 15$; paired *t*-test), including a representation of axial, limb, and orolingual scores using different shades (Two-way ANOVA, Bonferroni's test; Rater: $F_{(1,42)} = 0.31$, $p = 0.58$; AIM subtype: $F_{(2,42)} = 29.28$; $p < 0.001$; Interaction: $F_{(2,42)} = 1.95$, $p = 0.15$). **B** and **C**. Time course of basic scores and amplitude scores, respectively, within the same test session. The corresponding sums of scores are shown in **B′** and **C′**, respectively. Axial, limb, and orolingual components are represented using different shades. No significant differences between raters were found on any of these parameters.

1998) previously found to blunt AIM scores in this mouse model (Lundblad et al., 2005). Data from both raters were concordant in showing a significant reduction in global AIM scores by amantadine (Fig. 3). The magnitude of the effect was larger when using the combined global scale compared to either unidimensional scale (Fig. 3 and Table 3). Amantadine had a stronger effect on time-based AIM scores compared to amplitude scores (cf. Fig. 3B and C, and Table 3), although it significantly affected both dimensions.

No significant difference between rater #1 and #2 scores was found on either basic, amplitude or global scores during amantadine challenge test (correlation between raters: Fig. 3A′, Global AIMs: $r^2 = 0.94$, $p < 0.001$; Fig. 3B′, Basic AIMs: $r^2 = 0.90$, $p < 0.001$; Fig. 3C′, Amplitude AIMs: $r^2 = 0.91$, $p < 0.001$). Moreover, there was a high concordance between raters regarding the antidyskinetic effect of amantadine on the three topographic subtypes of AIMs, which appeared to be equally affected (Fig. 3A′, B′, C′).

3.2. Effects of the D1R antagonist SCH23390

SCH23390 (SCH) is a widely used antagonist of D1 class DARs. In this study, the doses of 0.05 and 0.125 mg/kg (SCH 0.05 and SCH 0.125) were chosen based on observations of effects in previous studies using C57Bl/6 mice (Svenningsson et al., 2000; Santini et al., 2009a; Santini et al., 2009b). The two doses of SCH produced a similar reduction in global AIM scores (Fig. 4A′, −64% and −61% for 0.05 and 0.125 mg/kg doses; $p < 0.001$ vs. veh + L-DOPA). Similar effects were seen also when considering basic AIM scores (Fig. 4B, −50% and −48% for 0.05 and 0.125 mg/kg doses; $p < 0.001$ vs. veh + L-DOPA), and amplitude scores per se (Fig. 4C, −49% for both 0.05 and 0.125 mg/kg doses; $p < 0.001$ vs. veh + L-DOPA).

The effects of SCH on L-DOPA-induced general motor activity were evaluated by testing the mice in an automated open field apparatus. The time course of horizontal activity, vertical activity, contralateral turns and ipsilateral turns are shown in Fig. 4D, E, F, G, respectively. Total counts recorded over 140 min after L-DOPA injection are shown in Fig. 4D′, E′, F′ and G′.

The profile of L-DOPA-induced horizontal activity had four phases: (i) a transient increase around 10 min post L-DOPA injection, before the appearance of dyskinetic movements (Fig. 4D, +283%, $p < 0.001$ vs. baseline); (ii) a dip in distance travelled between 15 and 100 min post L-DOPA injection, corresponding to the time when animals were highly affected by dyskinesia; (iii) a second rise between 100 and 125 min, which corresponded to the time when AIMs levels were decreasing, and (iv) a decline between 125 and 140 min. During this last interval mice were free from AIMs and gradually resumed their normal resting state. Analysis of the total counts revealed that L-DOPA had induced a dramatic increase in total distance travelled during the test session (Fig. 4D′, +1046%, $p < 0.001$ vs. baseline). Coadministration of L-DOPA and SCH 0.05 led to an increase in total distance travelled similar to that induced by L-DOPA monotreatment (Fig. 4D′, +1221%, $p < 0.001$ vs. baseline). On the other hand, the higher dose of SCH (0.125 mg/kg) reduced the total distance travelled compared to both L-DOPA monotreatment and the combination of L-DOPA and SCH 0.05 (Fig. 4D′, −51%, $p < 0.01$ vs. veh + L-DOPA. -57%, $p < 0.001$ vs. SCH 0.05 + L-DOPA).

Vertical activity was quantified as number of rearing events during the test session, which showed a temporal course similar to the distance travelled (Fig. 4E). The total number of rearing events increased after treatment with either L-DOPA (Fig. 4E′, +1895%, $p < 0.001$ vs. baseline), or L-DOPA plus SCH 0.05 (Fig. 4E′, +1077%, $p < 0.05$ vs. baseline). However, the higher dose of SCH (0.125 mg/kg) inhibited the effect of L-DOPA on the number of rearing events (Fig. 4E′, −89%; $p < 0.001$ vs. veh + L-DOPA; non-significant difference vs. baseline values).

Animals receiving a unilateral 6-OHDA lesion show an ipsilateral rotational bias at baseline, but rotate towards the side contralateral to the lesion after treatment with L-DOPA (Ungerstedt, 1968, 1971). As expected, mice injected with L-DOPA, alone or combined with either dose of SCH, displayed increased number of contralateral rotations (Fig. 4F′, $p < 0.001$ for all treatments vs. baseline). However, cotreatment with SCH 0.125 and L-DOPA significantly reduced the number of contralateral rotations compared to both L-DOPA monotreatment and L-DOPA plus SCH 0.05 (Fig. 4F′, −60%, $p < 0.01$ vs. veh + L-DOPA, and −65%; $p < 0.01$ vs. SCH 0.05 + L-DOPA). Fig. 4G and G′ depict the counts of ipsilateral rotations (much lower than the contralateral ones, as expected; see Francardo et al., 2011; Bez et al., 2016). The number of ipsilateral rotations showed a short peak 5 min after the injection

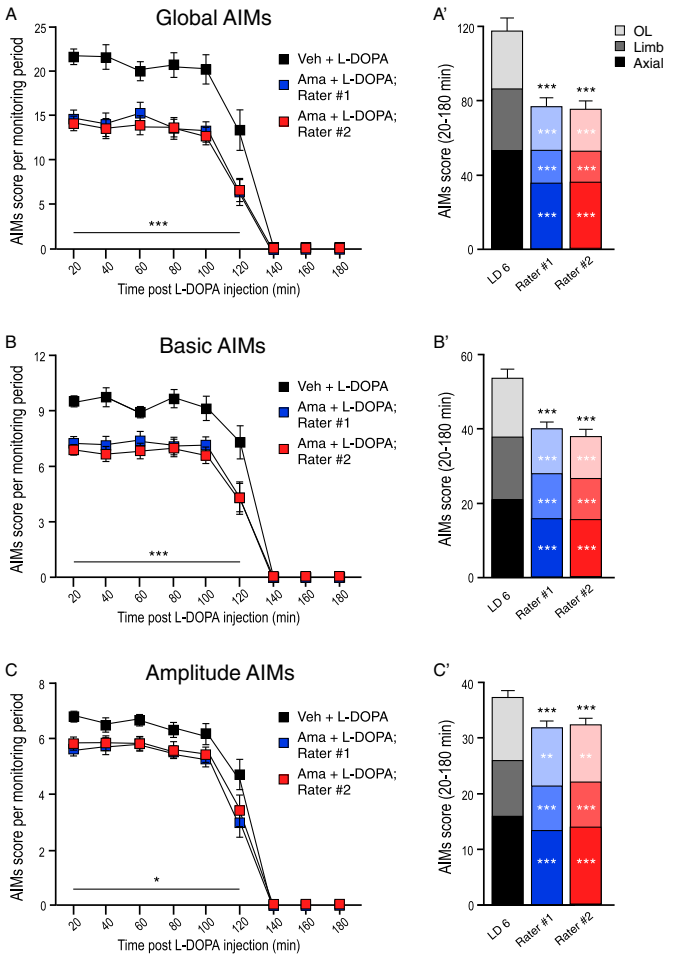

Fig. 3. Antidyskinetic effects of amantadine (Ama, 40 mg/kg) as detected by different raters and different scales. **A**. Time course of global AIM scores following an injection of 6 mg/kg L-DOPA, preceded by Ama or vehicle. Amantadine significantly attenuated the AIM scores from 20 to 120 min after L-DOPA injection regardless of the rater (RM Two-way ANOVA, Treatment: $F_{(2,28)} = 77.88$, $p < 0.001$; Time: $F_{(8,112)} = 128.7$, $p < 0.001$; Interaction: $F_{(16,224)} = 12.49$, $p < 0.001$). Post hoc Bonferroni's test: $p < 0.001$ for Ama + L-DOPA vs. veh + L-DOPA; $p > 0.05$ for data from the two raters. **A′**. The total global AIM score per test session shows a significant effect of amantadine (RM One-way ANOVA, Treatment: $F_{(2,28)} = 77.88$, $p < 0.001$), and no difference between raters on either the sum of axial, limb, and orolingual scores or each topographic AIM subtype (represented by color shades within the bars). **B**. Time course of basic AIM scores (RM Two-way ANOVA, Treatment: $F_{(2,28)} = 67.07$, $p < 0.001$; Time: $F_{(8,112)} = 150.7$, $p < 0.001$; Interaction: $F_{(16,224)} = 9.84$, $p < 0.001$). **B′**. Total scores for basic AIMs (RM One-way ANOVA, Treatment: $F_{(2,28)} = 67.07$, $p < 0.001$). **C**. Time course of amplitude AIM scores (RM Two-way ANOVA, Treatment: $F_{(2,28)} = 35.14$, $p < 0.001$; Time: $F_{(8,112)} = 267.0$, $p < 0.001$; Interaction: $F_{(16,224)} = 3.92$, $p < 0.001$). **C′**. Total scores for amplitude AIMs (RM One-way ANOVA, Treatment: $F_{(2,28)} = 35.14$, $p < 0.001$). Results from post-hoc group comparisons (Bonferroni's test) are reported as follows: $^{*}p < 0.05$, $^{**}p < 0.01$ and $^{***}p < 0.001$ vs. veh + L-DOPA, respectively. Significances represented by white asterisks refer to the change on the given topographic score.

of L-DOPA, remained very low between 15 and 100 min, and tended to rise again at the end of the recording session (Fig. 4G). The counts recorded upon treatment with L-DOPA, alone or combined with SCH 0.05, were not statistically different from baseline values. However, when L-DOPA was combined with the higher dose of SCH, a significant reduction in ipsilateral rotations was detected compared to all other conditions (Fig. 4G′, −48%, $p < 0.05$ vs. baseline; −54%, $p < 0.01$ vs. veh + L-DOPA, and −39%, $p < 0.01$ vs. SCH 0.05 + L-DOPA). The effects of SCH on L-DOPA-induced horizontal, vertical, and rotational activities are summarized in Table 4, which also enables comparisons with the effects produced by the other DAR antagonists.

3.3. Effects of the D2R antagonist Raclopride

Raclopride (Rac) is a D2-class DAR antagonist with low nanomolar affinity for both D2 and D3 receptors. The doses of 0.05 and 0.250 mg/kg (Rac 0.05 and Rac 0.250) were selected based on previous literature (Santini et al., 2009a). The compound dose-dependently reduced dyskinesia severity throughout the test session (Fig. 5A). Global AIM scores were significantly reduced by both doses of Rac, although the larger dose was more effective (Fig. 5A′, Rac 0.05 + L-DOPA: −59%, $p < 0.001$ vs. veh + L-DOPA; Rac 0.250 + L-DOPA: −69%, $p < 0.001$ vs. veh + L-DOPA, and −25%, $p < 0.05$ vs. Rac 0.05 + L-DOPA). Significant effects of Rac were detected also upon analysis of basic AIM scores and amplitude scores per se, although the effect was less pronounced than that on global AIMs (cf. Table 3). Thus, Rac 0.05 and 0.250 mg/kg reduced basic AIM scores by 49% and 58%, respectively (Fig. 5B, $p < 0.001$ for both doses vs. veh + L-DOPA, and $p < 0.05$ for Rac 0.250 + L-DOPA vs. Rac 0.05 + L-DOPA). Amplitude scores were reduced by 40% and 55%, respectively (Fig. 5C, $p < 0.001$ for both drug doses vs. veh + L-DOPA and $p < 0.01$ for Rac 0.250 + L-DOPA vs. Rac 0.05 + L-DOPA).

Paralleling the reduction in dyskinesia severity, treatment with either dose of Rac increased the total distance travelled compared to both baseline and L-DOPA treatment (Fig. 5D′, Rac 0.05 + L-DOPA: +1535%, $p < 0.001$ vs. baseline, and +43%, $p < 0.01$ vs. veh + L-DOPA; Rac 0.250 + L-DOPA: +1582%, $p < 0.001$ vs. baseline, and +47%, $p < 0.01$ vs. veh + L-DOPA).

Counts of rearing events were increased compared to baseline by both doses of Rac in combination with L-DOPA (Fig. 5E′, Rac 0.05 + L-DOPA: +1776% $p < 0.001$ vs. baseline; Rac 0.250 + L-DOPA: +1396%, $p < 0.01$ vs. baseline) and did not differ significantly from the values recorded after treatment with L-DOPA only.

Cotreating mice with Rac 0.05 and 0.125 mg/kg and L-DOPA led to an increased number of contralateral rotations similar to that produced by L-DOPA only (Fig. 5F′, Rac 0.05 + L-DOPA and Rac 0.250 + L-DOPA: ~300-fold increase, $p < 0.001$ vs. baseline). Mice performed comparable levels of ipsilateral rotations upon all treatment conditions, but for Rac 0.250 and L-DOPA cotreatment, which resulted in a mild reduction (Fig. 5G′, −27%, $p < 0.05$ vs. Rac 0.05 + L-DOPA).

3.4. Effects of the D3R antagonist PG01037

PG01037 is a selective D3R antagonist already tested in rodent models of LID. For the present study we selected the doses of 3 and 10 mg/kg (PG 3 and PG 10) based on the documented *in vivo* D3R binding activity of the lower dose (Higley et al., 2011) and the reported antidyskinetic activity of the higher dose (Solis et al., 2015). The D3R antagonist dose-dependently reduced global AIM scores throughout the dyskinesia-time curve (Fig. 6A) and both doses of PG had a significant effect (Fig. 6A′, PG 3 + L-DOPA: −38%, $p < 0.001$ vs. veh + L-DOPA; PG 10 + L-DOPA: −48%, $p < 0.001$ vs. veh + L-DOPA). Basic AIM scores were also significantly blunted by both the low and the high dose (Fig. 6B, reductions by 22% and 32%, respectively, $p < 0.001$ vs. veh + L-DOPA). Interestingly however, the lower dose of PG failed to reduce amplitude AIM scores, while the higher dose yielded a 28% decrease (Fig. 6C, $p < 0.001$ vs. both veh + L-DOPA, and PG 3 + L-DOPA).

After challenge with the lower dose of PG, total distance travelled did not differ significantly from that recorded upon L-DOPA monotreatment. On the other hand, the higher dose of PG increased the total distance travelled to a level higher than all other treatment conditions (Fig. 6D′, +1790%, $p < 0.001$ vs. baseline; +65%, $p < 0.001$ vs. veh + L-DOPA, and +45%, $p < 0.001$ vs. PG 3 + L-DOPA).

The total number of rearings was increased by both PG doses (Fig. 6E′, PG 3 + L-DOPA: +2390%, $p < 0.001$ vs. baseline; PG 10 + L-DOPA: +4013%, $p < 0.001$ vs. baseline). The higher dose of PG produced a number of rearings significantly greater than L-DOPA-only treatment

Table 3
Effects of amantadine and DAR antagonists on global, basic and amplitude AIMs.

Main target receptor	Compound	Dose	Effect on global AIMs	Effect on basic AIMs	Effect on amplitude AIMs
NMDAR	Amantadine	40 mg/kg	−36%	−28%	−15%
D1R/D5R	SCH23390	0.05 mg/kg	−64%	−50%	−49%
		0.125 mg/kg	−61%	−48%	−49%
D2R/D3R	Raclopride	0.05 mg/kg	−59%	−49%	−40%
		0.250 mg/kg	−69%	−58%	−55%
D3R	PG01037	3 mg/kg	−38%	−22%	0.03%
		10 mg/kg	−48%	−32%	−28%
D4R	L-745,870	1 mg/kg	−26%	−12%	−16%
		3 mg/kg	−35%	−22%	−19%
D4R	VU6004461	10 mg/kg	−59%	−44%	−39%
		20 mg/kg	−71%	−55%	−44%

The effect refers to the average reduction in ALO scores per session (20–180 min) upon administration of the compound with L-DOPA, relative to L-DOPA pus vehicle (cf. Fig. 3A′, B′, C′ and Figs. 4A′–C, 5A′–C, 6′–C, 7A′–C, 8A′–C). For amantadine, the mean % change of scores from rater #1 and rater #2 is reported.

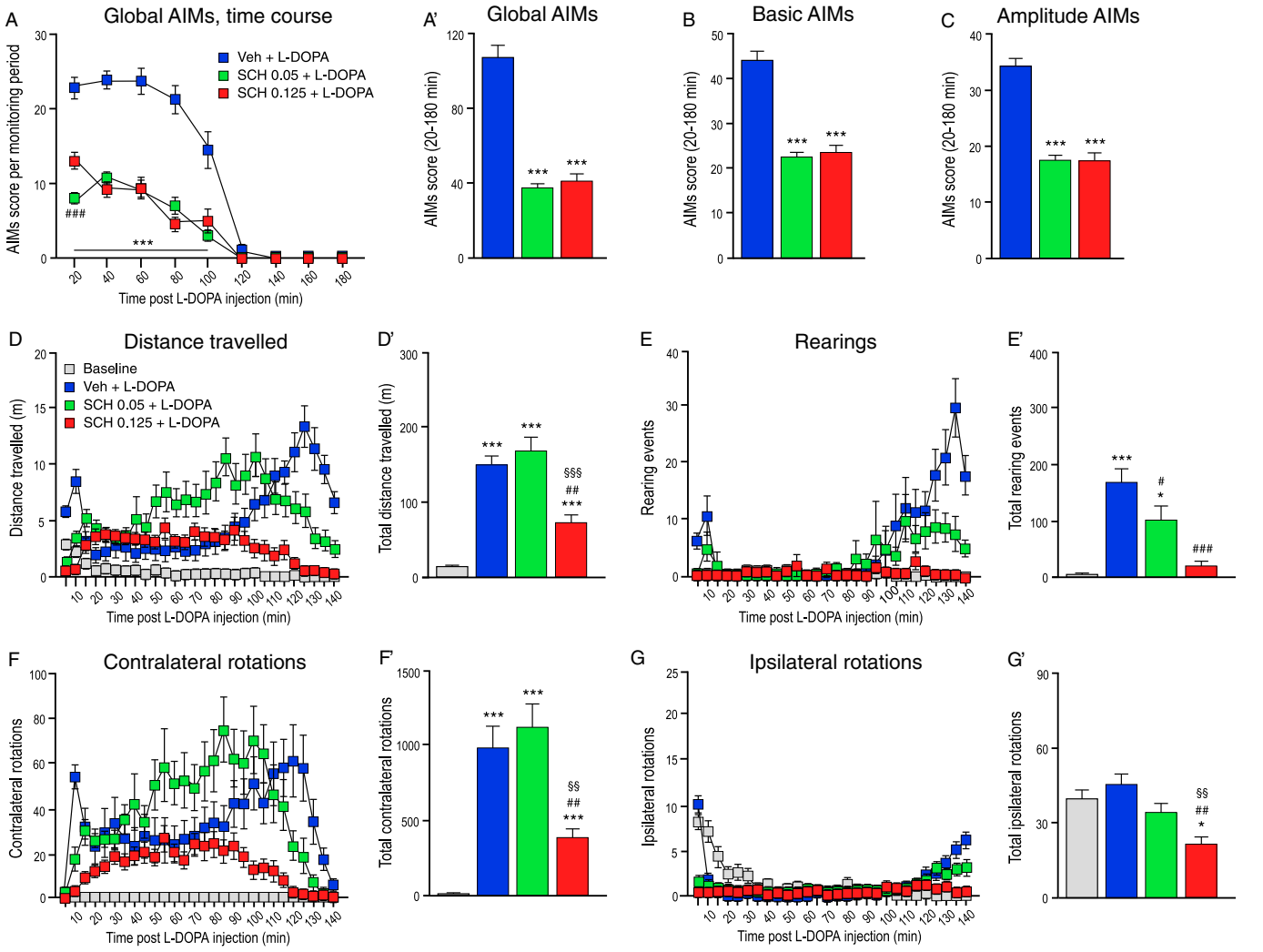

Fig. 4. Effects of the D1R antagonist, SCH23390 (SCH) tested at the doses of 0.05 and 0.125 mg/kg. (A–C) Effects on L-DOPA-induced AIMs, (D–G′) effects of changes in horizontal, vertical and rotational activity induced by L-DOPA (open field test). **A**. Time course of global AIM scores (RM Two-way ANOVA, Treatment: $F_{(2,28)} = 103.6$, $p < 0.001$; Time point: $F_{(8,112)} = 128.6$, $p < 0.001$; Interaction $F_{(16,224)} = 24.28$, $p < 0.001$). **A′**. Total scores for global AIMs (RM One-way ANOVA, Treatment: $F_{(2,28)} = 103.6$, $p < 0.001$). **B**. Total scores for basic AIMs (RM One-way ANOVA, Treatment: $F_{(2,28)} = 88.46$, $p < 0.001$). **C**. Total scores for amplitude AIMs (RM One-way ANOVA, Treatment: $F_{(2,28)} = 74.67$, $p < 0.001$). Results from post-hoc group comparisons (Bonferroni's test) are reported as follows: $^{***}p < 0.001$ vs. veh + L-DOPA; $^{###}p < 0.001$ vs. SCH 0.125 + L-DOPA. **D**. Time course of distance travelled (RM Two-way ANOVA, Treatment: $F_{(3,42)} = 40.46$, $p < 0.001$; Time: $F_{(27,378)} = 3.8$, $p < 0.001$; Interaction $F_{(81,1134)} = 9.93$, $p < 0.001$). **D′**. Total distance travelled (RM One-way ANOVA, Treatment: $F_{(3,42)} = 40.46$, $p < 0.001$). **E**. Time course of rearing events (RM Two-way ANOVA, Treatment: $F_{(3,42)} = 21.79$, $p < 0.001$; Time: $F_{(27,378)} = 9.19$, $p < 0.001$; Interaction $F_{(81,1134)} = 6.01$, $p < 0.001$). **E′**. Total number of rearing events (RM One-way ANOVA, Treatment: $F_{(3,42)} = 21.79$, $p < 0.001$). **F**. Time course of contralateral rotations (RM Two-way ANOVA, Treatment: $F_{(3,42)} = 29.68$, $p < 0.001$; Time: $F_{(27,378)} = 6.98$, $p < 0.001$; Interaction $F_{(81,1134)} = 4.31$, $p < 0.001$). **F′**. Total number of contralateral rotations (RM One-way ANOVA, Treatment: $F_{(3,42)} = 29.68$, $p < 0.001$). **G**. Time course of ipsilateral rotations (RM Two-way ANOVA, Treatment: $F_{(3,42)} = 8.23$, $p < 0.001$; Time: $F_{(27,378)} = 22.54$, $p < 0.001$; Interaction $F_{(81,1134)} = 11.68$, $p < 0.001$). **G′**. Total number of ipsilateral rotations (RM One-way ANOVA, Treatment: $F_{(3,42)} = 8.23$, $p < 0.001$). Results from post-hoc group comparisons (Bonferroni's test) are reported as follows: $^{*}p < 0.05$ and $^{***}p < 0.001$ vs. baseline, respectively; $^{\#}p < 0.05$, $^{\#\#}p < 0.01$ and $^{\#\#\#}p < 0.001$ vs. veh + L-DOPA, respectively; $^{\S\S}p < 0.01$ and $^{\S\S\S}p < 0.001$ vs. SCH 0.05 + L-DOPA.

(Fig. 6E′, +106%, $p < 0.05$ vs. veh + L-DOPA). Mice challenged with both doses of PG displayed an increased number of contralateral rotations, tending to exceed the effect of L-DOPA monotreatment, although the difference did not reach statistical significance (Fig. 6F′, PG 3 + L-DOPA: +11%, $p > 0.05$ vs. veh + L-DOPA; PG 10 + L-DOPA: +31%, $p > 0.05$ vs. veh + L-DOPA). No significant differences were detected regarding total number of ipsilateral rotations (Fig. 6G′).

3.5. Effects of the D4R antagonist L-745,870

L-745,870 is a D4R antagonist reported to improve LID in both macaque (Huot et al., 2012) and rat models (Huot et al., 2014), and the doses of 1 and 3 mg/kg (L-7 1 and L-7 3) were chosen based on these previous publications. Global AIM scores were dose-dependently reduced by L-7 throughout the dyskinesia-time curve (Fig. 7A). Accordingly, the global scores per session were significantly reduced by both drug doses (Fig. 7A′, L-7 1 + L-DOPA: −26%, $p < 0.001$ vs. veh + L-DOPA; L-7 3 + L-DOPA: −35%, $p < 0.001$ vs. veh + L-DOPA). Both doses of L-7 had a significant, though modest effect on basic AIM scores (Fig. 7B, L-7 1 + L-DOPA: −12%, $p < 0.01$ vs. veh + L-DOPA; L-7 3 + L-DOPA: −22%, $p < 0.01$ vs. veh + L-DOPA), and similarly reduced the amplitude scores (Fig. 7C, L7 1 + L-DOPA: −16%, $p < 0.001$ vs. veh + L-DOPA; L-7 3 + L-DOPA: −19%, $p < 0.01$ vs. veh + L-DOPA).

The analysis of horizontal activity revealed that either dose of L-7 markedly increased the total distance travelled compared to baseline, but the difference from L-DOPA monotreatment only reached significance with the dose of 1 mg/kg (Fig. 7D′, L-7 1 + L-DOPA: +1445%, $p < 0.001$ vs. baseline, and +35%, $p < 0.05$ vs. veh + L-DOPA; L-7 3 + L-DOPA: +1409%, $p < 0.001$ vs. baseline).

Rearings were markedly increased compared to baseline by both doses of L-7, but only 1 mg/kg L-7 induced significantly more rearings than L-DOPA monotreatment (Fig. 7E′, L-7 1 + L-DOPA: +3197%, $p < 0.001$ vs. baseline, and +65% $p < 0.05$ vs. veh + L-DOPA; L-7 3 + L-DOPA: +3188%, $p < 0.001$ vs. baseline).

Contralateral rotations induced by either L-7 dose were not significantly different than after L-DOPA monotreatment (Fig. 7F′, L-7 1 + L-DOPA: ~310-fold increase, $p < 0.001$ vs. baseline; L-7 3 + L-DOPA: ~270-fold increase, $p < 0.001$ vs. baseline). No significant difference in the total number of ipsilateral rotation was found when comparing the different treatment conditions.

3.6. Effects of the novel D4R antagonist VU6004461

VU6004461 is a novel D4R antagonist, selective and highly brain penetrable, recently synthetized at the Vanderbilt Center for Neuroscience Drug Discovery (Witt et al., 2016) and never previously tested on animal models of PD or LID. The doses of 10 and 20 mg/kg (VU 10 and VU 20) were chosen based on *in vivo* pharmacokinetic data provided by Vanderbilt Center for Neuroscience Drug Discovery. VU6004461 potently reduced global AIM scores per monitoring period throughout the entire dyskinesia-time curve (Fig. 8A). Global scores per session were dramatically reduced by both doses of VU (Fig. 8A′, VU 10 + L-DOPA: −59%, $p < 0.001$ vs. veh + L-DOPA; VU 20 + L-DOPA: −71%, $p < 0.001$ vs. veh + L-DOPA). Basic scores were decreased in a dose-dependent manner (Fig. 8B, VU 10 + L-DOPA: −44%, $p < 0.001$ vs. veh + L-DOPA; VU 20 + L-DOPA: −55%, $p < 0.001$ vs. veh + L-DOPA, and −19%, $p < 0.05$ vs. VU 10 + L-DOPA). However, when amplitude AIM scores were considered, the two VU doses had comparable efficacy (Fig. 8C, VU 10 + L-DOPA: −39%, $p < 0.001$ vs. veh + L-DOPA; VU 20 + L-DOPA: −44%, $p < 0.001$ vs. veh + L-DOPA).

Cotreatment with VU and L-DOPA induced a large increase in total distance travelled, similar to that induced by L-DOPA monotreatment (Fig. 8D′, VU 10 + L-DOPA: +1367%, $p < 0.001$ vs. baseline; VU 20 + L-DOPA: +1408%, $p < 0.001$ vs. baseline).

The total number of rearings was similarly incremented by both VU doses when compared to baseline, and the effect was similar to that produced by L-DOPA only (Fig. 8E′, VU 10 + L-DOPA: +3329%, $p < 0.001$ vs. baseline; VU 20 + L-DOPA: +3351%, $p < 0.001$ vs. baseline).

Mice treated with either dose of VU showed high levels of contralateral rotation (Fig. 8E, E′), although the difference from L-DOPA monotreatment did not reach significance (Fig. 8F′). However, counts of ipsilateral rotations were higher after challenge with VU, and the difference from L-DOPA monotreatment reached significance with the lower VU dose (Fig. 8G′, VU 10 + L-DOPA: +69%, $p < 0.01$ vs. baseline, and +47%, $p < 0.05$ vs. veh + L-DOPA; VU 20 + L-DOPA: +60%, $p < 0.05$ vs. baseline).

4. Discussion

The first aim of this study was to develop and validate a sensitive method for assessing LID in the mouse, similar to the one currently used in the rat (Rylander et al., 2010; Breger et al., 2013; Iderberg et al., 2013; Iderberg et al., 2015). Our results show that a dyskinesia scale combining a time dimension with an amplitude dimension can be accurately applied to the mouse model of LID by well-trained investigators. Moreover, this scale was more sensitive than unidimensional scales in detecting antidyskinetic effects of pharmacological agents (Table 3). The second aim of this study was to evaluate the antidyskinetic efficacy of subtype-specific DAR antagonists, also including a novel D4R antagonist never previously tested in any animal model of PD or LID. Although the role of D1Rs in LID is well established (Westin et al., 2007; Darmopil et al., 2009), an increasing number of reports indicate that other types of DARs also are implicated, including DAR subtypes having low levels of expression in the striatum (Bordet et al., 1997; Kumar et al., 2009; Huot et al., 2012; Huot et al., 2014; Solis et al., 2015). We therefore set out to compare the relative ability of selective D1-type, D2-type, D3 and D4 receptor antagonists to modulate LID using the new rating scale.

4.1. Methodological considerations

The assessment of dyskinesia in both PD patients and non-human primate models of PD is based on rating scales that consider the duration, body distribution and disabling character of the involuntary movements. Similar principles have inspired the development of rating scales for both rodent and non-human primate models of LID. Although automated methods are being developed to assess LID severity (Griffiths et al., 2012; Tsipouras et al., 2012), rating scales will remain necessary to capture the complexity of the movement disorder and its qualitative characteristics.

In current mouse models of LID, the most common assessment method is the basic AIM scale first introduced by Cenci and collaborators (Lundblad et al., 2004), which defines LID severity based on the proportion of observation time during which different topographic subtypes of AIMs are present. This scale has been well validated and it is widely used to assess candidate antidyskinetic interventions (Pavon et al., 2006; Santini et al., 2007; Bateup et al., 2010). Our results confirm that this scale is sufficiently sensitive to detect pharmacologically induced changes in dyskinesia severity. However, a limitation of this scale is that it fails to discriminate between large and fine movements. This may not be a problem when the relationship between frequency and amplitude of dyskinesia is fixed and predictable. However, this feature is not known a priori when testing antidyskinetic treatments, nor when establishing new animal models of LID. For example, we have previously found that the amplitude of both axial and limb AIMs is generally smaller when LID is induced in rodents with partial striatal 6-OHDA lesions compared to complete lesions (Winkler et al., 2002; Francardo et al., 2011). The utility of combining a time-based scale with one sensitive to changes in dyskinesia 'amplitude' was highlighted by some recent studies, which introduced assessments of movement amplitude in the evaluation of pro-dyskinetic or anti-dyskinetic interventions

Table 4
Modulation of L-DOPA-induced changes in motor activity by tested treatments.

	SCH 0.05 mg/kg	SCH 0.125 mg/kg	Rac 0.05 mg/kg	Rac 0.250 mg/kg	PG 3 mg/kg	PG 10 mg/kg	L-7 1 mg/kg	L-7 3 mg/kg	VU 10 mg/kg	VU 20 mg/kg
Total distance travelled	+15%	−51%**	+43%**	+47%**	+13%	+65%***	+35%*	+32%	+28%	+32%
Total contralateral rotations	+13%	−60%**	+9%	+8%	+11%	+31%	+13%	−1%	+18%	+20%
Total rearings	−41%*	−89%***	−6%	−25%	+25%	+106%*	+65%*	+65%	+72%	+73%
Total ipsilateral rotations	−25%	−54%**	+8%	−22%	−11%	+1%	+60%	+32%	+47%*	+39%

Compounds were given in combination with L-DOPA. Data report the percentage change relative to the values recorded after L-DOPA plus vehicle. All values refer to data recorded during a 140 min recording session. Abbreviations: SCH: SCH23390; Rac: Raclopride; PG: PG01037; L-7: L-745,870; VU: VU6004461. Results from post-hoc group comparisons (Bonferroni's test) are reported as follows: *p < 0.05, **p < 0.01 and ***p < 0.001 vs. veh + L-DOPA, respectively.

(Smith et al., 2012; Bordia et al., 2016). However, our scale is the first to clearly define amplitude grades from 1 to 4 for each of the main topographic subtypes of dyskinesia in the mouse. The strikingly similar scores provided by independent raters prove that the scale is well-anchored to objective criteria. It should, however, be pointed out that the two raters involved had acquired extensive previous training on the rat global AIM scale. Before applying the global AIM scale to the mouse, it may therefore be useful to learn how to rate AIMs amplitude

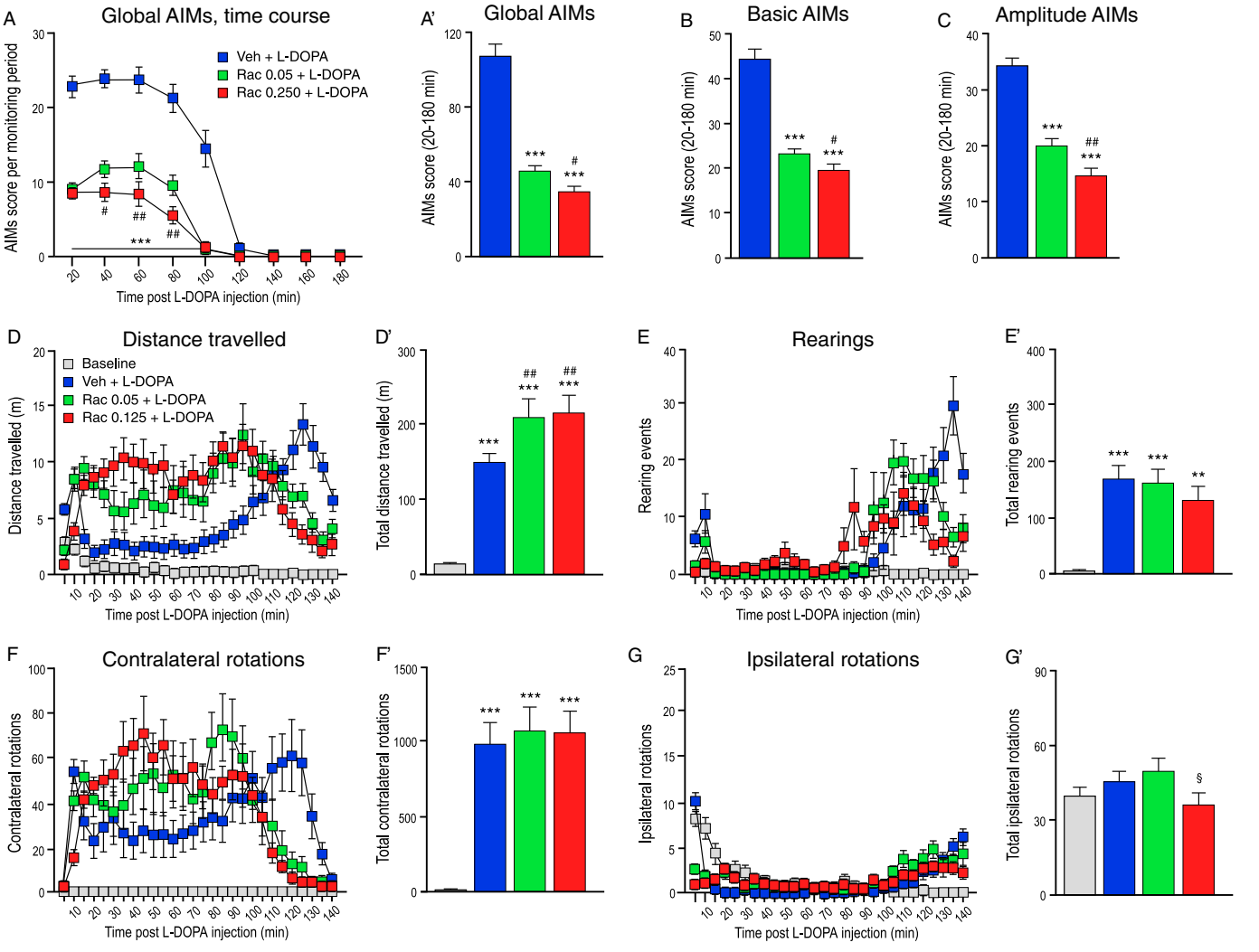

Fig. 5. Effects of the D2R antagonist, Raclopride (Rac) tested at the doses of 0.05 and 0.250 mg/kg. (A–C) Effects on L-DOPA-induced AIMs, (D–G′) effects of changes in horizontal, vertical and rotational activity induced by L-DOPA (open field test). **A**. Time course of global AIM scores (RM Two-way ANOVA, Treatment: $F_{(2,28)} = 140.8$, $p < 0.001$; Time: $F_{(8,112)} = 130.6$, $p < 0.001$; Interaction $F_{(16,224)} = 24.46$, $p < 0.001$). **A′**. Total scores for global AIMs (RM One-way ANOVA, Treatment: $F_{(2,28)} = 140.8$, $p < 0.001$). **B**. Total scores for basic AIMs (RM One-way ANOVA, Treatment: $F_{(2,28)} = 157.7$, $p < 0.001$). **C**. Total scores for amplitude AIMs (RM One-way ANOVA, Treatment: $F_{(2,28)} = 108.1$, $p < 0.001$). Results from post-hoc group comparisons (Bonferroni's test) are reported as follows: ***p < 0.001 vs. veh + L-DOPA; #p < 0.05 and ##p < 0.01 vs. Rac 0.05 + L-DOPA, respectively. **D**. Time course of distance travelled (RM Two-way ANOVA, Treatment: $F_{(3,42)} = 47.30$, $p < 0.001$; Time: $F_{(27,378)} = 2.64$, $p < 0.001$; Interaction $F_{(81,1134)} = 8.34$, $p < 0.001$). **D′**. Total distance travelled (RM One-way ANOVA, Treatment: $F_{(3,42)} = 47.30$, $p < 0.001$). **E**. Time course for rearing events (RM Two-way ANOVA, Treatment: $F_{(3,42)} = 22.35$, $p < 0.001$; Time: $F_{(27,378)} = 13.64$, $p < 0.001$; Interaction $F_{(81,1134)} = 6.41$, $p < 0.001$). **E′**. Total number of rearing events (RM One-way ANOVA, Treatment: $F_{(3,42)} = 22.35$, $p < 0.001$). **F**. Time course of contralateral rotations (RM Two-way ANOVA, Treatment: $F_{(3,42)} = 28.98$, $p < 0.001$; Time: $F_{(27,378)} = 5.72$, $p < 0.001$; Interaction $F_{(81,1134)} = 5.22$, $p < 0.001$). **F′**. Total number of contralateral rotations (RM One-way ANOVA, Treatment: $F_{(3,42)} = 28.98$, $p < 0.001$). **G**. Time course of ipsilateral rotations (RM Two-way ANOVA, Treatment: $F_{(3,42)} = 2.26$, $p < 0.05$; Time: $F_{(27,378)} = 19.87$, $p < 0.001$; Interaction $F_{(81,1134)} = 10.51$, $p < 0.001$). **G′**. Total number of ipsilateral rotations (RM One-way ANOVA, Treatment: $F_{(3,42)} = 2.26$, $p = 0.12$). Results from post-hoc group comparisons (Bonferroni's test) are reported as follows: **p < 0.01 and ***p < 0.001 vs. baseline, respectively; ##p < 0.01 vs. veh + L-DOPA; §p < 0.05 vs. Rac 0.05 + L-DOPA.

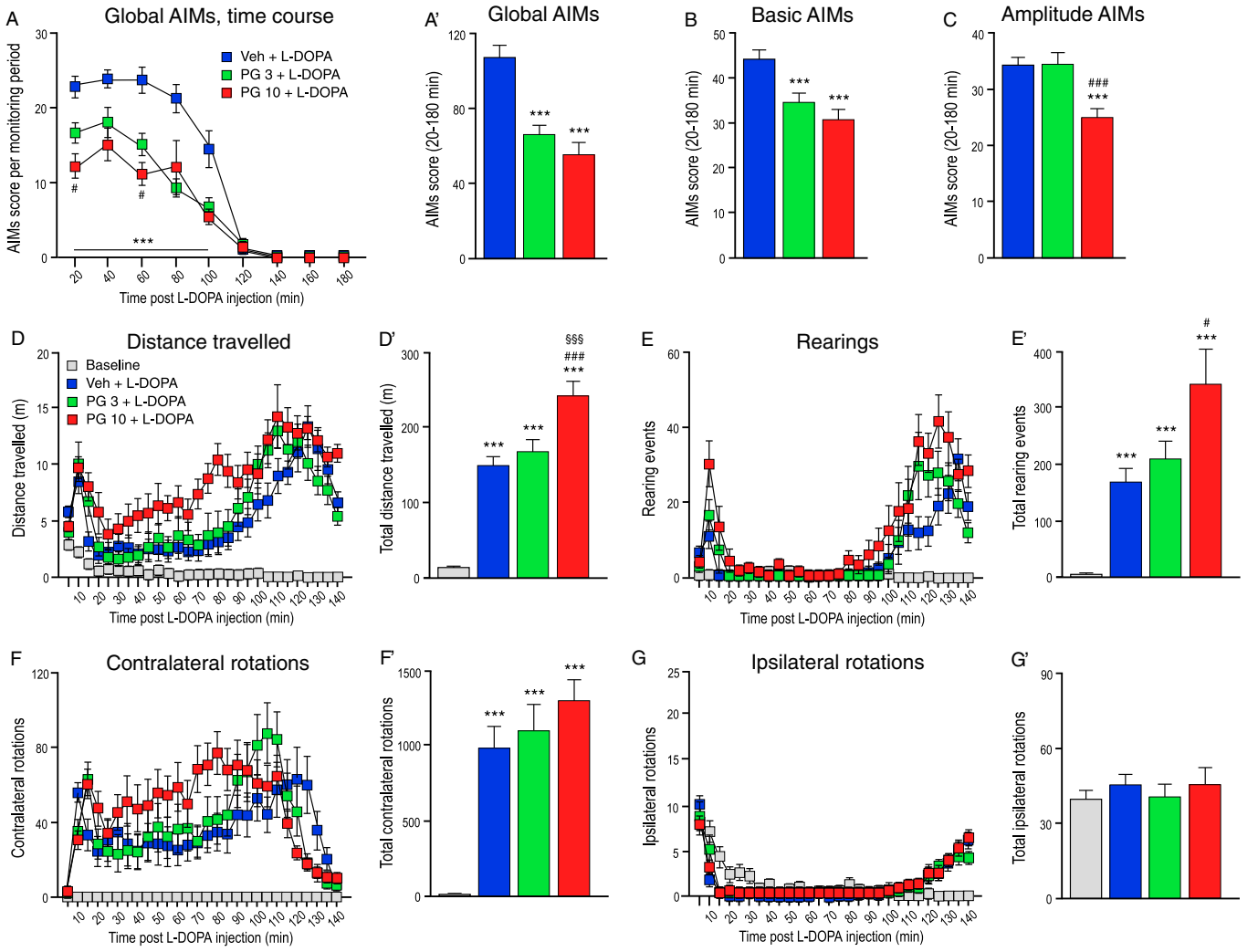

Fig. 6. Effects of the D3R antagonist, PG01037 (PG) tested at the doses of 3 and 10 mg/kg on LID. (A–C) Effects on L-DOPA-induced AIMs, (D–G′) effects of changes in horizontal, vertical and rotational activity induced by L-DOPA (open field test). **A**. Time course of global AIM scores (RM Two-way ANOVA, Treatment: $F_{(2,28)} = 42.95$, $p < 0.001$; Time: $F_{(8,112)} = 87.47$, $p < 0.001$; Interaction $F_{(16,224)} = 7.31$, $p < 0.001$). **A′**. Total scores for global AIMs (RM One-way ANOVA, Treatment: $F_{(2,28)} = 42.95$, $p < 0.001$). **B**. Total scores for basic AIMs (RM One-way ANOVA, Treatment: $F_{(2,28)} = 19.44$, $p < 0.001$). **C**. Total scores for amplitude AIMs (RM One-way ANOVA, Treatment: $F_{(2,28)} = 21.6$, $p < 0.001$). Results from post-hoc group comparisons (Bonferroni's test) are reported as follows: $^{***}p < 0.001$ vs. veh + L-DOPA; $^{\#}p < 0.05$ and $^{\#\#\#}p < 0.001$ vs. PG 3 + L-DOPA, respectively. **D**. Time course of distance travelled (RM Two-way ANOVA, Treatment: $F_{(3,42)} = 70.99$, $p < 0.001$; Time: $F_{(27,378)} = 14.41$, $p < 0.001$; Interaction $F_{(81,1134)} = 4.85$, $p < 0.001$). **D′**. Total distance travelled (RM One-way ANOVA, Treatment: $F_{(3,42)} = 70.99$, $p < 0.001$). **E**. Time course of rearing events (RM Two-way ANOVA, Treatment: $F_{(3,42)} = 20.57$, $p < 0.001$; Time: $F_{(27,378)} = 20.49$, $p < 0.001$; Interaction $F_{(81,1134)} = 6.31$, $p < 0.001$). **E′**. Total number of rearing events (RM One-way ANOVA, Treatment: $F_{(3,42)} = 20.57$, $p < 0.001$). **F**. Time course of contralateral rotations (RM Two-way ANOVA, Treatment: $F_{(3,42)} = 35.68$, $p < 0.001$; Time: $F_{(27,378)} = 6.68$, $p < 0.001$; Interaction $F_{(81,1134)} = 4.29$, $p < 0.001$). **F′**. Total number of contralateral rotations (RM One-way ANOVA, Treatment: $F_{(3,42)} = 35.68$, $p < 0.001$). **G**. Time course of ipsilateral rotations (RM Two-way ANOVA, Treatment: $F_{(3,42)} = 0.63$, $p = 0.59$; Time: $F_{(27,378)} = 47.16$, $p < 0.001$; Interaction $F_{(81,1134)} = 6.99$, $p < 0.001$). **G′**. Total number of ipsilateral rotations (RM One-way ANOVA, Treatment: $F_{(3,42)} = 0.63$, $p = 0.56$). Results from post-hoc group comparisons (Bonferroni's test) are reported as follows: $^{***}p < 0.001$ vs. baseline; $^{\#}p < 0.05$ and $^{\#\#\#}p < 0.001$ vs. veh + L-DOPA, respectively; $^{\S\S\S}p < 0.001$ vs. PG 3 + L-DOPA.

in the rat model of LID. Differences in AIMs amplitude are easier to distinguish in rat than mouse. Rats can engage in severe dyskinetic movements and postures for relatively long intervals (e.g. they can display an amplitude grade 3 in axial or in limb AIMs for longer than the 1 min observation time). On the contrary, mice have quicker and more variable movements, most often displaying a mixture of amplitude grades during the monitoring periods. Indeed, an important part of the validation work was to learn how to score AIMs amplitude in a consistent manner, and we resorted to using half points when the amplitude shifted between consecutive scores during the 1 min observation period. Video recordings proved very helpful for an off-line verification of the scores given on-line. Orolingual AIMs could be difficult to assess given the tendency of mice to cover the mouth with the dyskinetic forelimb. To circumvent this problem, we advise securing a good view of the mouse from below by using transparent cages and placing them on well-spaced metal beams. Additionally, it could be beneficial to perform extra observational sessions where investigators lift the animals up and specifically verify the amplitude of the orolingual AIMs, as illustrated by the pictures in Fig. 1.

In addition to developing a mouse global AIM scale, this study introduces a new complementary approach to evaluating antidyskinetic drug candidates using open field recordings of horizontal activity, vertical activity and rotational behavior. When studying unilateral models of LID, rotational behavior is commonly assessed in automated rotameter bowls, but this method yields results of difficult interpretation (Cenci et al., 2002; Iderberg et al., 2012). In our dataset, treatments increasing both distance travelled and contralateral rotations between 20 and 100 min post L-DOPA administration, invariably reduced AIM scores during the same interval. Thus, positive changes in distance travelled and contralateral rotation may verify the antidyskinetic efficacy of a treatment. Conversely, treatments that significantly reduce these activity measures may have a motor depressant effect (cf. effects of

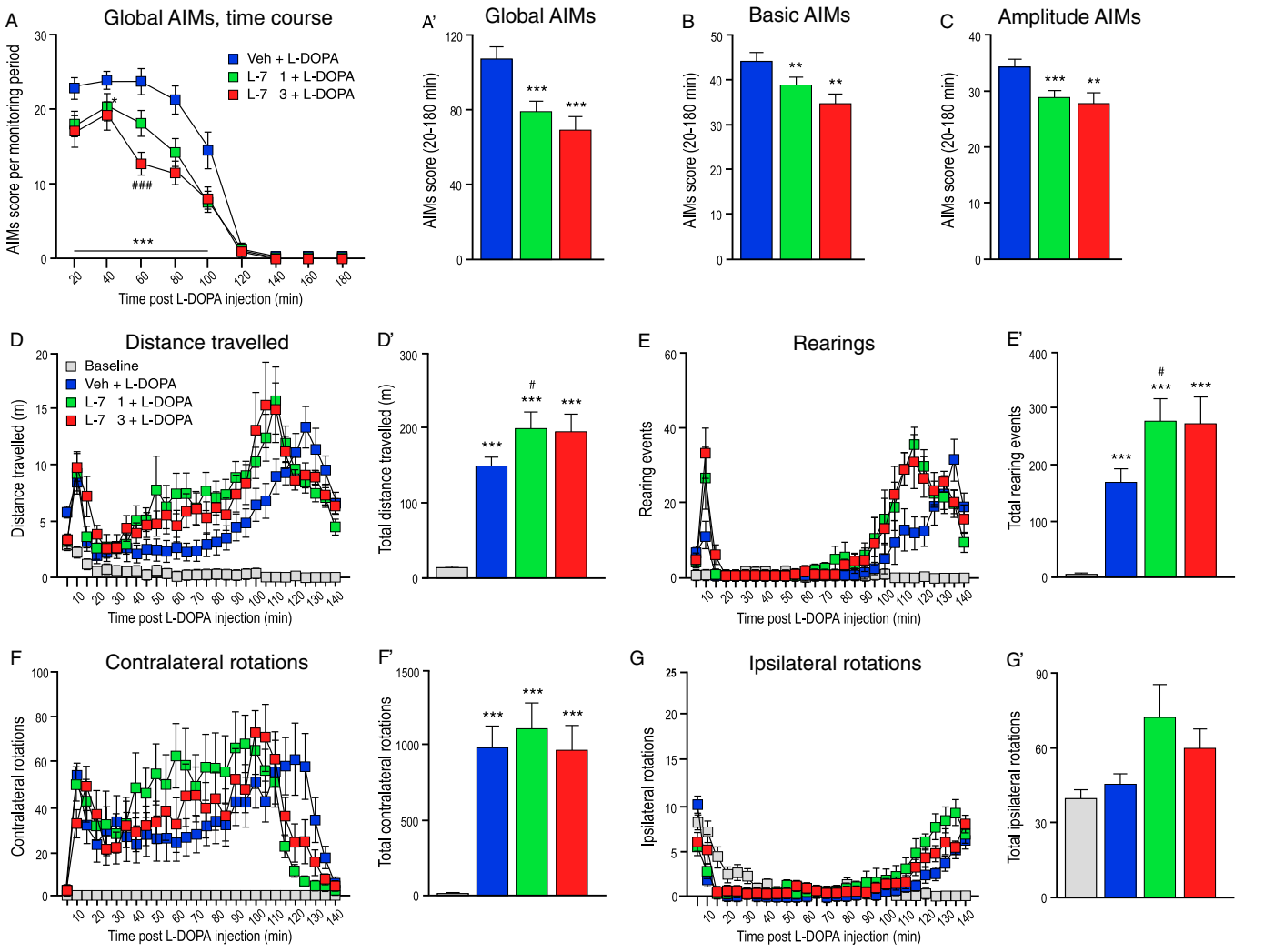

Fig. 7. Effects of the D4R antagonist, L-745,870 (L-7) tested at the doses of 1 and 3 mg/kg. (A–C) Effects on L-DOPA-induced AIMs, (D–G′) effects of changes in horizontal, vertical and rotational activity induced by L-DOPA (open field test). **A**. Time course of global AIM scores (RM Two-way ANOVA, Treatment: $F_{(2,28)} = 26.19$, $p < 0.001$; Time: $F_{(8,112)} = 122$, $p < 0.001$; Interaction $F_{(16,224)} = 6.29$, $p < 0.001$). **A′**. Total scores for global AIMs (RM One-way ANOVA, Treatment: $F_{(2,28)} = 26.19$, $p < 0.001$). **B**. Total scores for basic AIMs (RM One-way ANOVA, Treatment: $F_{(2,28)} = 15.89$, $p < 0.001$). **C**. Total scores for amplitude AIMs (RM One-way ANOVA, Treatment: $F_{(2,28)} = 16.67$, $p < 0.001$). Results from post-hoc group comparisons (Bonferroni's test) are reported as follows: $^{**}p < 0.01$ and $^{***}p < 0.001$ vs. veh + L-DOPA, respectively; $^{\#\#\#}p < 0.001$ vs. L-7 1 + L-DOPA. **D**. Time course of distance travelled (RM Two-way ANOVA, Treatment: $F_{(3,42)} = 44.53$, $p < 0.001$; Time: $F_{(27,378)} = 12.54$, $p < 0.001$; Interaction $F_{(81,1134)} = 5.31$, $p < 0.001$). **D′**. Total distance travelled (RM One-way ANOVA, Treatment: $F_{(3,42)} = 44.53$, $p < 0.001$). **E**. Time course of rearing events (RM Two-way ANOVA, Treatment: $F_{(3,42)} = 23.17$, $p < 0.001$; Time: $F_{(27,378)} = 19.80$, $p < 0.001$; Interaction $F_{(81,1134)} = 6.06$, $p < 0.001$). **E′**. Total number of rearing events (RM One-way ANOVA, Treatment: $F_{(3,42)} = 23.17$, $p < 0.001$). **F**. Time course of contralateral rotations (RM Two-way ANOVA, Treatment: $F_{(3,42)} = 26$, $p < 0.001$; Time: $F_{(27,378)} = 5.24$, $p < 0.001$; Interaction $F_{(81,1134)} = 3.55$, $p < 0.001$). **F′**. Total number of contralateral rotations (RM One-way ANOVA, Treatment: $F_{(3,42)} = 26.0$, $p < 0.001$). **G**. Time course of ipsilateral rotations (RM Two-way ANOVA, Treatment: $F_{(3,42)} = 3.67$, $p < 0.05$; Time: $F_{(27,378)} = 32.62$, $p < 0.001$; Interaction $F_{(81,1134)} = 9.25$, $p < 0.001$). **G′**. Total number of ipsilateral rotations (RM One-way ANOVA, Treatment: $F_{(3,42)} = 3.67$, $p < 0.05$). Results from post-hoc group comparisons (Bonferroni's test) are reported as follows: $^{***}p < 0.001$ vs. baseline; $^{\#}p < 0.05$ vs. veh + L-DOPA.

SCH23390 0.125 mg/kg, Table 4). Thus, automated recordings of horizontal, vertical, and rotational activity in an open field can provide a simple method to explore the therapeutic window of potential antidyskinetic treatments, i.e. the dose range at which a treatment counteracts LID without compromising the motor stimulant (antiakinetic) action of L-DOPA. Open field tests will not, however, obviate the need for analyzing specific motor endpoints that can better inform translation (Cenci et al., 2002; Iderberg et al., 2015; Pinna et al., 2016).

4.2. Evaluation of the antidyskinetic efficacy of DAR antagonists

DARs belong to the G protein-coupled receptors (GPCR) superfamily and based on their coupling to either $G\alpha_{s/olf}$ or $G\alpha_{i/o}$ proteins, they can be grouped into a D1-like or D2-like family, respectively (Sibley et al., 1993). The former includes D1R and D5R, which promote the production of cAMP; the latter includes D2R, D3R and D4R, which inhibit the production of cAMP. Different DAR subtypes have distinct anatomical distributions and they are pharmacological targets for multiple disorders affecting the central nervous system, including psychiatric disorders, PD and LID.

Among all DARs, the D1 type has a well-proven role in LID. Genetic ablation of the D1R completely prevents the development of LID in the mouse (Darmopil et al., 2009), and altered signaling responses downstream of D1R are causally linked with LID development in both rodent and non-human primate models (reviewed in Cenci and Konradi, 2010). SCH23390 is a potent D1R/D5 antagonist ($K_i = 0.2$ and 0.3 nM for D1R and D5R, respectively; Bourne, 2001), centrally active after systemic administration. In rat models of LID, SCH23390 exerts pronounced antidyskinetic effects (Monville et al., 2005; Westin et al., 2007). This effect is accompanied by an inhibition of striatal signaling responses that are strongly associated with LID, such as the phosphorylation of extracellular signal-regulated kinases 1 and 2 (ERK1/2)

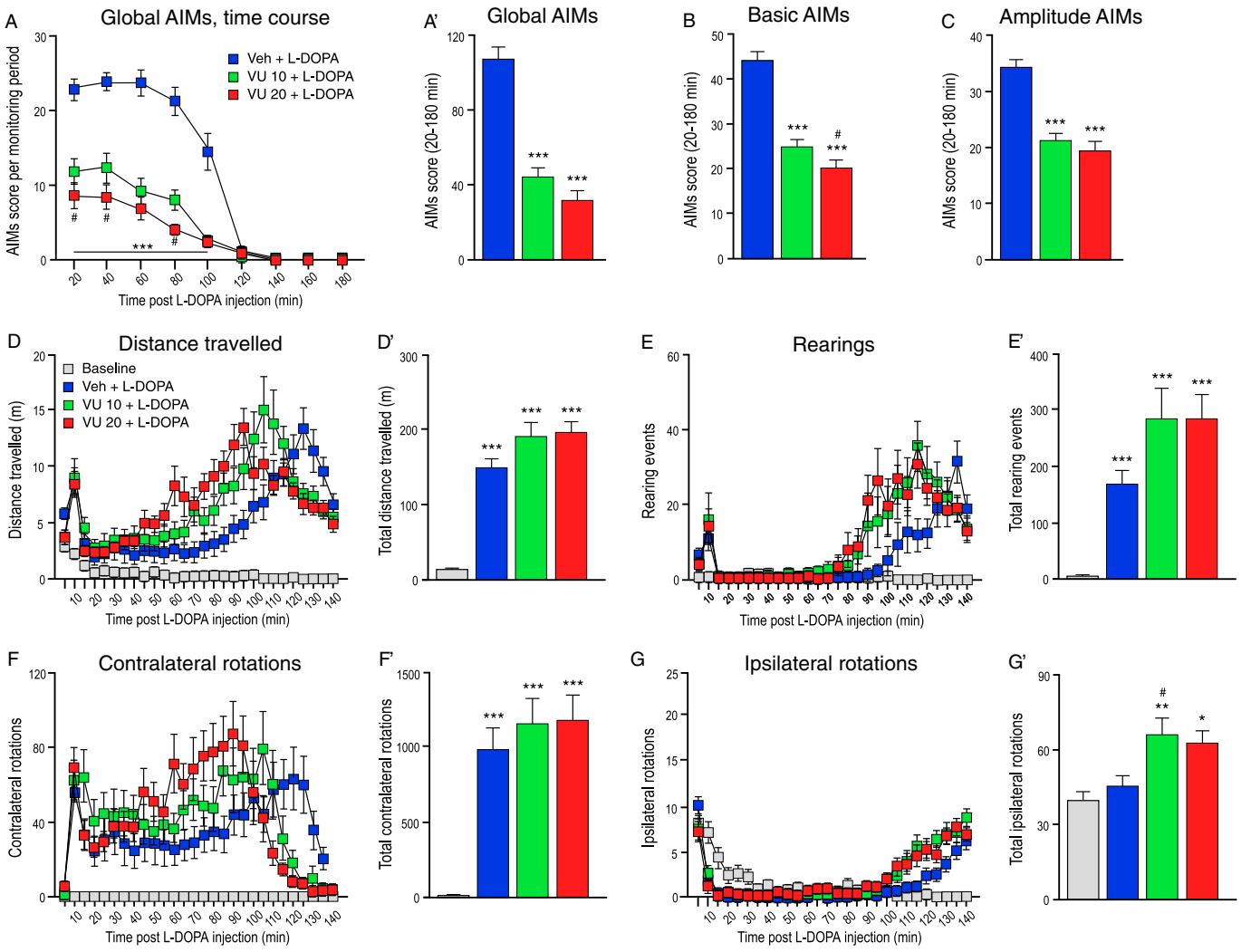

Fig. 8. Effects of the selective D4R antagonist, VU6004461 (VU) tested at the doses of 10 and 20 mg/kg on LID. (A–C) Effects on L-DOPA-induced AIMs, (D–G′) effects of changes in horizontal, vertical and rotational activity induced by L-DOPA (open field test). **A**. Time course of global AIM scores (RM Two-way ANOVA, Treatment: $F_{(2,28)} = 88.10$, $p < 0.001$; Time: $F_{(8,112)} = 96.44$, $p < 0.001$; Interaction $F_{(16,224)} = 20.64$, $p < 0.001$). **A′**. Total scores for global AIMs (RM One-way ANOVA, Treatment: $F_{(2,28)} = 88.10$, $p < 0.001$). **B**. Total scores for basic AIMs (RM One-way ANOVA, Treatment: $F_{(2,28)} = 78.32$, $p < 0.001$). **C**. Total scores for amplitude AIMs (RM One-way ANOVA, Treatment: $F_{(2,28)} = 56.68$, $p < 0.001$). Results from post-hoc group comparisons (Bonferroni's test) are reported as follows: ***$p < 0.001$ vs. veh + L-DOPA; #$p < 0.05$ vs. VU 10 + L-DOPA. **D**. Time course of distance travelled (RM Two-way ANOVA, Treatment: $F_{(3,42)} = 43.33$, $p < 0.001$; Time: $F_{(27,378)} = 18.44$, $p < 0.001$; Interaction $F_{(81,1134)} = 6.61$, $p < 0.001$). **D′**. Total distance travelled (RM One-way ANOVA, Treatment: $F_{(3,42)} = 43.33$, $p < 0.001$). **E**. Time course of rearing events (RM Two-way ANOVA, Treatment: $F_{(3,42)} = 12.77$, $p < 0.001$; Time: $F_{(27,378)} = 19.18$, $p < 0.001$; Interaction $F_{(81,1134)} = 4.43$, $p < 0.001$). **E′**. Total number of rearing events (RM One-way ANOVA, Treatment: $F_{(3,42)} = 12.77$, $p < 0.001$). **F**. Time course of contralateral rotations (RM Two-way ANOVA, Treatment: $F_{(3,42)} = 19.78$, $p < 0.001$; Time: $F_{(27,378)} = 9.96$, $p < 0.001$; Interaction $F_{(81,1134)} = 4.41$, $p < 0.001$). **F′**. Total number of contralateral rotations (RM One-way ANOVA, Treatment: $F_{(3,42)} = 19.78$, $p < 0.001$). **G**. Time course of ipsilateral rotations (RM Two-way ANOVA, Treatment: $F_{(3,42)} = 6.92$, $p < 0.001$; Time: $F_{(27,378)} = 46.07$, $p < 0.001$; Interaction $F_{(81,1134)} = 9.51$, $p < 0.001$). **G′**. Total number of ipsilateral rotations (RM One-way ANOVA, Treatment: $F_{(3,42)} = 6.92$, $p < 0.01$). Results from post-hoc group comparisons (Bonferroni's test) are reported as follows: *$p < 0.05$, **$p < 0.01$ and ***$p < 0.001$ vs. baseline, respectively; #$p < 0.05$ vs. veh + L-DOPA.

(Westin et al., 2007; Santini et al., 2009a; Fieblinger et al., 2014b), and the upregulation of FosB/ΔFosB, a molecular marker of LID in both rodent (Andersson et al., 1999; Andersson et al., 2001) and non-human primate models (Berton et al., 2009). In our study, SCH23390 strikingly reduced all types of L-DOPA-induced AIMs at the doses of 0.05 and 0.125 mg/kg and had a dose-dependent impact on horizontal and vertical activity. While the lower dose of SCH23390 (0.05 mg/kg) increased both horizontal activity and contralateral rotations, the higher drug dose (SCH23390 0.125 mg/kg) led to a decrease in all measures of L-DOPA-induced activity (distance travelled, rearings, contra- and ipsilateral rotations). These findings suggest inhibition of the therapeutic effect of L-DOPA by the higher dose of SCH (not however shared by the lower dose).

Notwithstanding the critical role of D1R, there are reports that D2R/D3R antagonists improve LID in 6-OHDA-lesioned rats (Delfino et al., 2004; Bagetta et al., 2012; Shin et al., 2012). We therefore tested Raclopride, a potent D2/D3 receptor antagonist (Ki = 1.8 and 3.5 nM for D2R and D3R, respectively; Kohler et al., 1985) previously found effective in the rat model of LID (Monville et al., 2005). Raclopride was found to markedly reduce all type of AIM scores in a dose-dependent manner. In line with a disengagement from dyskinesia, measures of general motor activity (distance travelled, rearings and contralateral rotations) were improved after combined treatment with Raclopride and L-DOPA. In our study, equivalent doses of SCH23390 and Raclopride (0.05 mg/kg) led to reductions of similar magnitude in all AIM scores, pointing to a concurrent role of D1R/D5R and D2R/D3R in the genesis of dyskinesia in the mouse.

In the rat model of LID, repeated L-DOPA injections lead to an induction of D3R gene expression in the dorsal striatum, mainly within D1R-expressing neurons (Bordet et al., 2000). Moreover, the development of

rotational sensitization to L-DOPA can be blocked by the D3R antagonist Nafadotride (Bordet et al., 1997). Binding sites for D2R and D3R have a high degree of homology. Therefore, we set out to test the highly selective D3R antagonist, PG01037 (Ki = 0.7 nM for D3R and 93.3 nM for D2R; Higley et al., 2011). Previous studies using PG01037 at the dose of 10 mg/kg have reported a reduction of L-DOPA-induced AIM scores in both MFB-lesioned rats (Kumar et al., 2009) and mice with striatal 6-OHDA lesions (Solis et al., 2015). To the best of our knowledge, antidyskinetic effects of 3 mg/kg PG01037 (a dose more suitable to antagonize the D3R only; Higley et al., 2011) have thus far not been reported. We found that 10 mg/kg PG01037 significantly reduced all types of AIM scores, leading to a parallel increase in horizontal and vertical activity, and contralateral rotations. However, 3 mg/kg PG01037 significantly reduced global and basic AIM scores, but left amplitude scores unaffected. Taken together, these data show that the antidyskinetic effects produced by the selective D3R antagonist PG01037 are more partial than those induced by the D2R/D3R antagonist Raclopride (which was fully effective already at the low dose of 0.05 mg/kg). These results therefore point to a significant contribution of D2Rs to the induction of dyskinesia by L-DOPA.

The D4R has been pursued as target for the treatment of schizophrenia (partly because of its high affinity for clozapine, see Van Tol et al. 1991) and several other neuropsychiatric conditions. Recent studies have shown that the selective D4R antagonist L-745,870 (Ki = 0.43 nM for D4R and 960 nM for D2R; Patel et al., 1997) improves LID in both MPTP-lesioned macaques and 6-OHDA-lesioned rats at the dose of 1 mg/kg (Huot et al., 2012; Huot et al., 2014). At the same dose, L-745,870 produced quite a modest reduction in both basic scores and amplitude scores (−12% and −16%, respectively), and a more clear-cut effect on the global AIM scores (−26%). The higher dose of L-745,870 (3 mg/kg) had slightly better effects. Changes in the open-field activity induced by L-DOPA were either not affected or slightly potentiated by L-745,870.

We also investigated the effect of a novel selective D4R antagonist, VU6004461 (Ki = 14.3 nM for D4R and 2400 nM for D2R; Witt et al., 2016), having high blood-brain barrier penetrability. VU6004461 induced a dose-dependent reduction in both basic and amplitude AIM scores. Global AIM scores were markedly improved by both doses of VU6004461. Along with a disengagement from dyskinesia, mice showed trends towards an increased horizontal and vertical activity compared to L-DOPA monotreatment. The clear antidyskinetic effect of both L-745,870 and VU6004461 point to the D4R as a possible future target for the treatment of LID, even though the treatment's mechanisms of action are currently unknown.

The striatum is not generally regarded as the primary site of action of D4R antagonists in neuropsychiatric conditions. Although detectable (Surmeier et al., 1996; Ariano et al., 1997), striatal expression levels of D4R are low. A study based on reverse transcription PCR has found D4R mRNA to be expressed in a subset of striatal projection neurons (Surmeier et al., 1996), but the functional significance of this finding has remained unexplored. However, one study has reported increased striatal levels of D4R binding following MFB lesion in the rat (Zhang et al., 2001). Brain regions expressing the highest levels of D4R in both rodents and non-human primates are the frontal cortex and limbic system (Mrzljak et al., 1996; Ariano et al., 1997). Abnormal oscillatory activities in the motor cortex have been recently linked to LID in both rat models (Halje et al., 2012) and human PD patients (Swann et al., 2016). These oscillatory activities involve cortical GABAergic interneurons (Halje et al., 2012; Swann et al., 2016), which have been shown to express the D4R (Mrzljak et al., 1996). Moreover, D4Rs are expressed in deep basal ganglia nuclei, such as the pallidum, substantia nigra reticulata and subthalamic nucleus (Mrzljak et al., 1996; Mauger et al., 1998; Flores et al., 1999; Rivera et al., 2002). These nuclei are engaged in pathological oscillatory activities in LID (reviewed in Bastide et al., 2015). These considerations highlight a need for investigating the role of D4Rs in pathological cortico-basal ganglia oscillations at the basis of LID.

In summary, our behavioral-pharmacological data indicate that antagonizing each main DAR subtype results in antidyskinetic effects in the mouse model of LID. There are however clear differences among the compounds here tested regarding both potency of the antidyskinetic action, and modulatory effects on L-DOPA-induced horizontal, vertical and rotational activities. Eventually, the utility of DAR antagonists to the treatment of LID will be determined by the balance between antidyskinetic potency and untoward effects.

4.3. Concluding remarks

Currently, a limited number of antidyskinetic treatments have made it to the clinic and the quest for drugs to reduce or abolish LID (without compromising the beneficial effects of DA replacement therapy) remains open. In order to preclinically characterize the effects of potential treatments, it is advantageous to develop rating scales that are anchored to objective physical parameters. We show here that this goal can be achieved by incorporating 'amplitude scores' and 'basic scores' into a global rating scale. The basic AIMs scale remains a valuable tool for evaluating potential antidyskinetic drugs in the mouse model of LID. Indeed, significant effects of all tested compounds were detected already by this scale. However, specific treatments may differentially impact on the frequency versus the amplitude of AIMs. Thus, there is an added value to evaluating both variables. This will allow for better unveiling subtle effects otherwise not visible with the sole use of the basic scale.

Funding

This study was supported by grants from the Swedish Governmental Funding of Clinical Research (ALF grant 43301) and the Swedish Research Council (VR 521-2011-2994, to MAC), and from the Michael J. Fox Foundation for Parkinson's Research (Grant ID: 10000, to CRH).

Acknowledgments

The authors are thankful to Dr. Anna Blobaum of the Vanderbilt Center of Neuroscience Drug Discovery for the pharmacokinetic studies on VU6004461. We also warmly thank Bengt Mattsson for the fine artwork that depicts amplitude AIM scores in Fig. 1; Laura Andreoli for sharing representative videos; Ann-Christin Lindh and Lindsay Einarsson for excellent technical assistance.

References

Ahlskog, J.E., Muenter, M.D., 2001. Frequency of levodopa-related dyskinesias and motor fluctuations as estimated from the cumulative literature. Mov. Disord. 16, 448–458.

Andersson, M., Hilbertson, A., Cenci, M.A., 1999. Striatal fosB expression is causally linked with L-DOPA-induced abnormal involuntary movements and the associated upregulation of striatal prodynorphin mRNA in a rat model of Parkinson's disease. Neurobiol. Dis. 6, 461–474.

Andersson, M., Konradi, C., Cenci, M.A., 2001. cAMP response element-binding protein is required for dopamine-dependent gene expression in the intact but not the dopamine-denervated striatum. J. Neurosci. 21, 9930–9943.

Ariano, M.A., Wang, J., Noblett, K.L., Larson, E.R., Sibley, D.R., 1997. Cellular distribution of the rat D4 dopamine receptor protein in the CNS using anti-receptor antisera. Brain Res. 752, 26–34.

Bagetta, V., Sgobio, C., Pendolino, V., Del Papa, G., Tozzi, A., Ghiglieri, V., Giampa, C., Zianni, E., Gardoni, F., Calabresi, P., Picconi, B., 2012. Rebalance of striatal NMDA/AMPA receptor ratio underlies the reduced emergence of dyskinesia during D2-like dopamine agonist treatment in experimental Parkinson's disease. J. Neurosci. 32, 17921–17931.

Bastide, M.F., Meissner, W.G., Picconi, B., Fasano, S., Fernagut, P.O., Feyder, M., Francardo, V., Alcacer, C., Ding, Y., Brambilla, R., Fisone, G., Jon Stoessl, A., Bourdenx, M., Engeln, M., Navailles, S., De Deurwaerdere, P., Ko, W.K., Simola, N., Morelli, M., Groc, L., Rodriguez, M.C., Gurevich, E.V., Quik, M., Morari, M., Mellone, M., Gardoni, F., Tronci, E., Guehl, D., Tison, F., Crossman, A.R., Kang, U.J., Steece-Collier, K., Fox, S., Carta, M., Angela Cenci, M., Bezard, E., 2015. Pathophysiology of L-DOPA-induced motor and non-motor complications in Parkinson's disease. Prog. Neurobiol. 132, 96–168.

Bateup, H.S., Santini, E., Shen, W., Birnbaum, S., Valjent, E., Surmeier, D.J., Fisone, G., Nestler, E.J., Greengard, P., 2010. Distinct subclasses of medium spiny neurons differentially regulate striatal motor behaviors. Proc. Natl. Acad. Sci. U. S. A. 107, 14845–14850.

Berton, O., Guigoni, C., Li, Q., Bioulac, B.H., Aubert, I., Gross, C.E., Dileone, R.J., Nestler, E.J., Bezard, E., 2009. Striatal overexpression of DeltaJunD resets L-DOPA-induced dyskinesia in a primate model of Parkinson disease. Biol. Psychiatry 66, 554–561.
Bez, F., Francardo, V., Cenci, M.A., 2016. Dramatic differences in susceptibility to L-DOPA-induced dyskinesia between mice that are aged before or after a nigrostriatal dopamine lesion. Neurobiol. Dis. 94, 213–225.
Bordet, R., Ridray, S., Carboni, S., Diaz, J., Sokoloff, P., Schwartz, J.C., 1997. Induction of dopamine D3 receptor expression as a mechanism of behavioral sensitization to levodopa. Proc. Natl. Acad. Sci. U. S. A. 94, 3363–3367.
Bordet, R., Ridray, S., Schwartz, J.C., Sokoloff, P., 2000. Involvement of the direct striatonigral pathway in levodopa-induced sensitization in 6-hydroxydopamine-lesioned rats. Eur. J. Neurosci. 12, 2117–2123.
Bordia, T., Perez, X.A., Heiss, J.E., Zhang, D., Quik, M., 2016. Optogenetic activation of striatal cholinergic interneurons regulates L-DOPA-induced dyskinesias. Neurobiol. Dis. 91, 47–58.
Bourne, J.A., 2001. SCH 23390: the first selective dopamine D1-like receptor antagonist. CNS Drug Rev. 7, 399–414.
Breger, L.S., Dunnett, S.B., Lane, E.L., 2013. Comparison of rating scales used to evaluate L-DOPA-induced dyskinesia in the 6-OHDA lesioned rat. Neurobiol. Dis. 50, 142–150.
Cenci, M.A., 2014. Glutamatergic pathways as a target for the treatment of dyskinesias in Parkinson's disease. Biochem. Soc. Trans. 42, 600–604.
Cenci, M.A., Konradi, C., 2010. Maladaptive striatal plasticity in L-DOPA-induced dyskinesia. Prog. Brain Res. 183, 209–233.
Cenci, M.A., Lundblad, M., 2006. Post- versus presynaptic plasticity in L-DOPA-induced dyskinesia. J. Neurochem. 99, 381–392.
Cenci, M.A., Lundblad, M., 2007. Ratings of L-DOPA-induced dyskinesia in the unilateral 6-OHDA lesion model of Parkinson's disease in rats and mice. Curr. Protoc. Neurosci. (Chapter **9**:Unit 9.25.1-9.25.23).
Cenci, M.A., Lee, C.S., Bjorklund, A., 1998. L-DOPA-induced dyskinesia in the rat is associated with striatal overexpression of prodynorphin- and glutamic acid decarboxylase mRNA. Eur. J. Neurosci. 10, 2694–2706.
Cenci, M.A., Whishaw, I.Q., Schallert, T., 2002. Animal models of neurological deficits: how relevant is the rat? Nat. Rev. Neurosci. 3, 574–579.
Cenci, M.A., Ohlin, K.E., Odin, P., 2011. Current options and future possibilities for the treatment of dyskinesia and motor fluctuations in Parkinson's disease. CNS Neurol. Disord. Drug Targets 10, 670–684.
Darmopil, S., Martin, A.B., De Diego, I.R., Ares, S., Moratalla, R., 2009. Genetic inactivation of dopamine D1 but not D2 receptors inhibits L-DOPA-induced dyskinesia and histone activation. Biol. Psychiatry 66, 603–613.
Delfino, M.A., Stefano, A.V., Ferrario, J.E., Taravini, I.R., Murer, M.G., Gershanik, O.S., 2004. Behavioral sensitization to different dopamine agonists in a parkinsonian rodent model of drug-induced dyskinesias. Behav. Brain Res. 152, 297–306.
Fieblinger, T., Graves, S.M., Sebel, L.E., Alcacer, C., Plotkin, J.L., Gertler, T.S., Chan, C.S., Heiman, M., Greengard, P., Cenci, M.A., Surmeier, D.J., 2014a. Cell type-specific plasticity of striatal projection neurons in parkinsonism and L-DOPA-induced dyskinesia. Nat. Commun. 5, 5316.
Fieblinger, T., Sebastianutto, I., Alcacer, C., Bimpisidis, Z., Maslava, N., Sandberg, S., Engblom, D., Cenci, M.A., 2014b. Mechanisms of dopamine D1 receptor-mediated ERK1/2 activation in the parkinsonian striatum and their modulation by metabotropic glutamate receptor type 5. J. Neurosci. 34, 4728–4740.
Flores, G., Liang, J.J., Sierra, A., Martinez-Fong, D., Quirion, R., Aceves, J., Srivastava, L.K., 1999. Expression of dopamine receptors in the subthalamic nucleus of the rat: characterization using reverse transcriptase-polymerase chain reaction and autoradiography. Neuroscience 91, 549–556.
Francardo, V., Recchia, A., Popovic, N., Andersson, D., Nissbrandt, H., Cenci, M.A., 2011. Impact of the lesion procedure on the profiles of motor impairment and molecular responsiveness to L-DOPA in the 6-hydroxydopamine mouse model of Parkinson's disease. Neurobiol. Dis. 42, 327–340.
Griffiths, R.I., Kotschet, K., Arfon, S., Xu, Z.M., Johnson, W., Drago, J., Evans, A., Kempster, P., Raghav, S., Horne, M.K., 2012. Automated assessment of bradykinesia and dyskinesia in Parkinson's disease. J. Parkinsons Dis. 2, 47–55.
Halje, P., Tamte, M., Richter, U., Mohammed, M., Cenci, M.A., Petersson, P., 2012. Levodopa-induced dyskinesia is strongly associated with resonant cortical oscillations. J. Neurosci. 32, 16541–16551.
Hauser, R.A., Rascol, O., Korczyn, A.D., Jon Stoessl, A., Watts, R.L., Poewe, W., De Deyn, P.P., Lang, A.E., 2007. Ten-year follow-up of Parkinson's disease patients randomized to initial therapy with ropinirole or levodopa. Mov. Disord. 22, 2409–2417.
Hechtner, M.C., Vogt, T., Zollner, Y., Schroder, S., Sauer, J.B., Binder, H., Singer, S., Mikolajczyk, R., 2014. Quality of life in Parkinson's disease patients with motor fluctuations and dyskinesias in five European countries. Parkinsonism Relat. Disord. 20, 969–974.
Higley, A.E., Spiller, K., Grundt, P., Newman, A.H., Kiefer, S.W., Xi, Z.X., Gardner, E.L., 2011. PG01037, a novel dopamine D3 receptor antagonist, inhibits the effects of methamphetamine in rats. J. Psychopharmacol. 25, 263–273.
Huot, P., Johnston, T.H., Koprich, J.B., Aman, A., Fox, S.H., Brotchie, J.M., 2012. L-745,870 reduces L-DOPA-induced dyskinesia in the 1-methyl-4-phenyl-1,2,3,6-tetrahydropyridine-lesioned macaque model of Parkinson's disease. J. Pharmacol. Exp. Ther. 342, 576–585.
Huot, P., Johnston, T.H., Koprich, J.B., Espinosa, M.C., Reyes, M.G., Fox, S.H., Brotchie, J.M., 2014. L-745,870 reduces the expression of abnormal involuntary movements in the 6-OHDA-lesioned rat. Behav. Pharmacol. 26, 101–108.
Iderberg, H., Francardo, V., Pioli, E.Y., 2012. Animal models of L-DOPA-induced dyskinesia: an update on the current options. Neuroscience 211, 13–27.
Iderberg, H., Rylander, D., Bimpisidis, Z., Cenci, M.A., 2013. Modulating mGluR5 and 5-HT1A/1B receptors to treat L-DOPA-induced dyskinesia: effects of combined treatment and possible mechanisms of action. Exp. Neurol. 250, 116–124.
Iderberg, H., Maslava, N., Thompson, A.D., Bubser, M., Niswender, C.M., Hopkins, C.R., Lindsley, C.W., Conn, P.J., Jones, C.K., Cenci, M.A., 2015. Pharmacological stimulation of metabotropic glutamate receptor type 4 in a rat model of Parkinson's disease and L-DOPA-induced dyskinesia: comparison between a positive allosteric modulator and an orthosteric agonist. Neuropharmacology 95, 121–129.
Kohler, C., Hall, H., Ogren, S.O., Gawell, L., 1985. Specific in vitro and in vivo binding of 3H-raclopride. A potent substituted benzamide drug with high affinity for dopamine D-2 receptors in the rat brain. Biochem. Pharmacol. 34, 2251–2259.
Kumar, R., Riddle, L., Griffin, S.A., Grundt, P., Newman, A.H., Luedtke, R.R., 2009. Evaluation of the D3 dopamine receptor selective antagonist PG01037 on L-DOPA-dependent abnormal involuntary movements in rats. Neuropharmacology 56, 944–955.
Lundblad, M., Andersson, M., Winkler, C., Kirik, D., Wierup, N., Cenci, M.A., 2002. Pharmacological validation of behavioural measures of akinesia and dyskinesia in a rat model of Parkinson's disease. Eur. J. Neurosci. 15, 120–132.
Lundblad, M., Picconi, B., Lindgren, H., Cenci, M.A., 2004. A model of L-DOPA-induced dyskinesia in 6-hydroxydopamine lesioned mice: relation to motor and cellular parameters of nigrostriatal function. Neurobiol. Dis. 16, 110–123.
Lundblad, M., Usiello, A., Carta, M., Hakansson, K., Fisone, G., Cenci, M.A., 2005. Pharmacological validation of a mouse model of L-DOPA-induced dyskinesia. Exp. Neurol. 194, 66–75.
Manson, A., Stirpe, P., Schrag, A., 2012. Levodopa-induced-dyskinesias clinical features, incidence, risk factors, management and impact on quality of life. J. Parkinsons Dis. 2, 189–198.
Mauger, C., Sivan, B., Brockhaus, M., Fuchs, S., Civelli, O., Monsma Jr., F., 1998. Development and characterization of antibodies directed against the mouse D4 dopamine receptor. Eur. J. Neurosci. 10, 529–537.
Metman, L.V., Del Dotto, P., van den Munckhof, P., Fang, J., Mouradian, M.M., Chase, T.N., 1998. Amantadine as treatment for dyskinesias and motor fluctuations in Parkinson's disease. Neurology 50, 1323–1326.
Monville, C., Torres, E.M., Dunnett, S.B., 2005. Validation of the L-DOPA-induced dyskinesia in the 6-OHDA model and evaluation of the effects of selective dopamine receptor agonists and antagonists. Brain Res. Bull. 68, 16–23.
Mrzljak, L., Bergson, C., Pappy, M., Huff, R., Levenson, R., Goldman-Rakic, P.S., 1996. Localization of dopamine D4 receptors in GABAergic neurons of the primate brain. Nature 381, 245–248.
Patel, S., Freedman, S., Chapman, K.L., Emms, F., Fletcher, A.E., Knowles, M., Marwood, R., McAllister, G., Myers, J., Curtis, N., Kulagowski, J.J., Leeson, P.D., Ridgill, M., Graham, M., Matheson, S., Rathbone, D., Watt, A.P., Bristow, L.J., Rupniak, N.M., Baskin, E., Lynch, J.J., Ragan, C.I., 1997. Biological profile of L-745,870, a selective antagonist with high affinity for the dopamine D4 receptor. J. Pharmacol. Exp. Ther. 283, 636–647.
Pavon, N., Martin, A.B., Mendialdua, A., Moratalla, R., 2006. ERK phosphorylation and FosB expression are associated with L-DOPA-induced dyskinesia in hemiparkinsonian mice. Biol. Psychiatry 59, 64–74.
Pinna, A., Ko, W.K., Costa, G., Tronci, E., Fidalgo, C., Simola, N., Li, Q., Tabrizi, M.A., Bezard, E., Carta, M., Morelli, M., 2016. Antidyskinetic effect of A2A and 5HT1A/1B receptor ligands in two animal models of Parkinson's disease. Mov. Disord. 31, 501–511.
Rivera, A., Cuellar, B., Giron, F.J., Grandy, D.K., de la Calle, A., Moratalla, R., 2002. Dopamine D4 receptors are heterogeneously distributed in the striosomes/matrix compartments of the striatum. J. Neurochem. 80, 219–229.
Rylander, D., Iderberg, H., Li, Q., Dekundy, A., Zhang, J., Li, H., Baishen, R., Danysz, W., Bezard, E., Cenci, M.A., 2010. A mGluR5 antagonist under clinical development improves L-DOPA-induced dyskinesia in parkinsonian rats and monkeys. Neurobiol. Dis. 39, 352–361.
Salat, D., Tolosa, E., 2013. Levodopa in the treatment of Parkinson's disease: current status and new developments. J. Parkinsons Dis. 3, 255–269.
Santini, E., Valjent, E., Usiello, A., Carta, M., Borgkvist, A., Girault, J.A., Herve, D., Greengard, P., Fisone, G., 2007. Critical involvement of cAMP/DARPP-32 and extracellular signal-regulated protein kinase signaling in L-DOPA-induced dyskinesia. J. Neurosci. 27, 6995–7005.
Santini, E., Alcacer, C., Cacciatore, S., Heiman, M., Herve, D., Greengard, P., Girault, J.A., Valjent, E., Fisone, G., 2009a. L-DOPA activates ERK signaling and phosphorylates histone H3 in the striatonigral medium spiny neurons of hemiparkinsonian mice. J. Neurochem. 108, 621–633.
Santini, E., Heiman, M., Greengard, P., Valjent, E., Fisone, G., 2009b. Inhibition of mTOR signaling in Parkinson's disease prevents L-DOPA-induced dyskinesia. Sci. Signal. 2, ra36.
Shin, E., Garcia, J., Winkler, C., Bjorklund, A., Carta, M., 2012. Serotonergic and dopaminergic mechanisms in graft-induced dyskinesia in a rat model of Parkinson's disease. Neurobiol. Dis. 47, 393–406.
Sibley, D.R., Monsma Jr., F.J., Shen, Y., 1993. Molecular neurobiology of dopaminergic receptors. Int. Rev. Neurobiol. 35, 391–415.
Smith, G.A., Heuer, A., Dunnett, S.B., Lane, E.L., 2012. Unilateral nigrostriatal 6-hydroxydopamine lesions in mice II: predicting L-DOPA-induced dyskinesia. Behav. Brain Res. 226, 281–292.
Solis, O., Garcia-Montes, J.R., Gonzalez-Granillo, A., Xu, M., Moratalla, R., 2015. Dopamine D3 receptor modulates L-DOPA-induced dyskinesia by targeting D1 receptor-mediated striatal signaling. Cereb. Cortex 1–12.
Surmeier, D.J., Song, W.J., Yan, Z., 1996. Coordinated expression of dopamine receptors in neostriatal medium spiny neurons. J. Neurosci. 16, 6579–6591.
Svenningsson, P., Lindskog, M., Ledent, C., Parmentier, M., Greengard, P., Fredholm, B.B., Fisone, G., 2000. Regulation of the phosphorylation of the dopamine- and cAMP-regulated phosphoprotein of 32 kDa in vivo by dopamine D1, dopamine D2, and adenosine A2A receptors. Proc. Natl. Acad. Sci. U. S. A. 97, 1856–1860.
Swann, N.C., de Hemptinne, C., Miocinovic, S., Qasim, S., Wang, S.S., Ziman, N., Ostrem, J.L., San Luciano, M., Galifianakis, N.B., Starr, P.A., 2016. Gamma oscillations in the

hyperkinetic state detected with chronic human brain recordings in Parkinson's disease. J. Neurosci. 36, 6445–6458.
Tsipouras, M.G., Tzallas, A.T., Rigas, G., Tsouli, S., Fotiadis, D.I., Konitsiotis, S., 2012. An automated methodology for levodopa-induced dyskinesia: assessment based on gyroscope and accelerometer signals. Artif. Intell. Med. 55, 127–135.
Ungerstedt, U., 1968. 6-Hydroxy-dopamine induced degeneration of central monoamine neurons. Eur. J. Pharmacol. 5, 107–110.
Ungerstedt, U., 1971. Postsynaptic supersensitivity after 6-hydroxy-dopamine induced degeneration of the nigro-striatal dopamine system. Acta Physiol. Scand. Suppl. 367, 69–93.
Van Tol, H.H., Bunzow, J.R., Guan, H.C., Sunahara, R.K., Seeman, P., Niznik, H.B., Civelli, O., 1991. Cloning of the gene for a human dopamine D4 receptor with high affinity for the antipsychotic clozapine. Nature 350, 610–614.
Westin, J.E., Lindgren, H.S., Gardi, J., Nyengaard, J.R., Brundin, P., Mohapel, P., Cenci, M.A., 2006. Endothelial proliferation and increased blood-brain barrier permeability in the basal ganglia in a rat model of 3,4-dihydroxyphenyl-L-alanine-induced dyskinesia. J. Neurosci. 26, 9448–9461.
Westin, J.E., Vercammen, L., Strome, E.M., Konradi, C., Cenci, M.A., 2007. Spatiotemporal pattern of striatal ERK1/2 phosphorylation in a rat model of L-DOPA-induced dyskinesia and the role of dopamine D1 receptors. Biol. Psychiatry 62, 800–810.
Winkler, C., Kirik, D., Bjorklund, A., Cenci, M.A., 2002. L-DOPA-induced dyskinesia in the intrastriatal 6-hydroxydopamine model of parkinson's disease: relation to motor and cellular parameters of nigrostriatal function. Neurobiol. Dis. 10, 165–186.
Witt, J.O., McCollum, A.L., Hurtado, M.A., Huseman, E.D., Jeffries, D.E., Temple, K.J., Plumley, H.C., Blobaum, A.L., Lindsley, C.W., Hopkins, C.R., 2016. Synthesis and characterization of a series of chiral alkoxymethyl morpholine analogs as dopamine receptor 4 (D4R) antagonists. Bioorg. Med. Chem. Lett. 26, 2481–2488.
Zhang, K., Tarazi, F.I., Baldessarini, R.J., 2001. Nigrostriatal dopaminergic denervation enhances dopamine D(4) receptor binding in rat caudate-putamen. Pharmacol. Biochem. Behav. 69, 111–116.